QEX

January/February 2022

www.arrl.org

A Forum for Communications Experimenters

Issue No. 330

WO9U creates custom keyboard interfaces.

The EVENT HORIZON OF DX

TS-990S

Dual TFT Display & Dual Receiver HF/50 MHz Transceiver

The main receiver has an IP3 in the +40 dB class, and the sub receiver is the already famous TS-590S receiver. Capable of receiving two signals at once, on different bands. 7-inch and 3.5-inch color TFT displays allow displaying of independent contents. Simplification of complex operations at a glance. Make no mistake, this is not a toy. Finally a serious tool is available for getting the very most from your hobby, of course it's a Kenwood.

- Covers the HF and 50 MHz bands.
- High-speed automatic antenna tuner.
- USB, Serial and LAN ports.
- Various PC applications (free software): ARCP-990 enabling PC control, ARHP-990 enabling remote control, and ARUA-10 USB audio driver.
- Clean 5 to 200 W transmit power through the 50 V FET final unit.
- Built-in RTTY and PSK.
- Three Analog Devices 32-bit floating-point arithmetic DSPs.
- DVI output for display by an external monitor (main screen display only).

KENWOOD

Customer Support: (310) 639-4200
Fax: (310) 537-8235

www.kenwood.com/usa

ISO9001 Registered

ADS#05421

QEX (ISSN: 0886-8093) is published bimonthly in January, March, May, July, September, and November by the American Radio Relay League, 225 Main St., Newington, CT 06111-1400. Periodicals postage paid at Hartford, CT and at additional mailing offices.

POSTMASTER: Send address changes to: QEX, 225 Main St., Newington, CT 06111-1400 Issue No. 330

Publisher
American Radio Relay League

Kazimierz "Kai" Siwiak, KE4PT
Editor

Lori Weinberg, KB1EIB
Assistant Editor

Scotty Cowling, WA2DFI
Ray Mack, W5IFS
Contributing Editors

Production Department

Becky R. Schoenfeld, W1BXY
Publications Manager

Michelle Bloom, WB1ENT
Production Supervisor

David Pingree, N1NAS
Senior Technical Illustrator

Brian Washing
Technical Illustrator

Advertising Information

Janet L. Rocco, W1JLR
Business Services
860-594-0203 – Direct
800-243-7768 – ARRL
860-594-4285 – Fax

Circulation Department

Cathy Stepina
QEX Circulation

Offices

225 Main St., Newington, CT 06111-1400 USA
Telephone: 860-594-0200
Fax: 860-594-0259 (24-hour direct line)
Email: **qex@arrl.org**

Subscription rate for 6 print issues:

In the US: $29

US by First Class Mail: $40;

International and Canada by Airmail: $35

ARRL members receive the digital edition of *QEX* as a member benefit.

In order to ensure prompt delivery, we ask that you periodically check the address information on your mailing label. If you find any inaccuracies, please contact the Circulation Department immediately. Thank you for your assistance.

January/February 2022

About the Cover

Tim Czerwonka, WO9U, uses Quantum Mechanical Keyboard (qmk) open-source microcontroller firmware to create customized keyboard interfaces. One interface is a simple rotary encoder with five programmable buttons and OLED display for use with a software-defined radio. The second is a commercial USB numeric keypad where he substituted his own microcontroller and firmware to achieve the desired programmability. The third is a 16-key macropad kit that would prove a quick and inexpensive keyboard addition in any ham shack. The qmk firmware offers a simple platform to generate key combinations with custom hardware that can simplify many software or radio tasks.

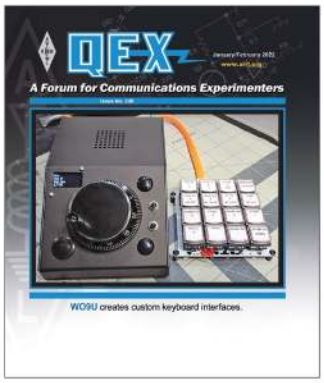

In This Issue

Index of Advertisers

The American Radio Relay League

The American Radio Relay League, Inc., is a noncommercial association of radio amateurs, organized for the promotion of interest in Amateur Radio communication and experimentation, for the establishment of networks to provide communications in the event of disasters or other emergencies, for the advancement of the radio art and of the public welfare, for the representation of the radio amateur in legislative matters, and for the maintenance of fraternalism and a high standard of conduct.

ARRL is an incorporated association without capital stock chartered under the laws of the state of Connecticut, and is an exempt organization under Section 501(c)(3) of the Internal Revenue Code of 1986. Its affairs are governed by a Board of Directors, whose voting members are elected every three years by the general membership. The officers are elected or appointed by the Directors. The League is noncommercial, and no one who could gain financially from the shaping of its affairs is eligible for membership on its Board.

"Of, by, and for the radio amateur," ARRL numbers within its ranks the vast majority of active amateurs in the nation and has a proud history of achievement as the standard-bearer in amateur affairs.

A *bona fide* interest in Amateur Radio is the only essential qualification of membership; an Amateur Radio license is not a prerequisite, although full voting membership is granted only to licensed amateurs in the US.

Membership inquiries and general correspondence should be addressed to the administrative headquarters:

ARRL
225 Main St.
Newington, CT 06111 USA
Telephone: 860-594-0200
FAX: 860-594-0259 (24-hour direct line)

Officers

President: Rick Roderick, K5UR
P.O. Box 1463, Little Rock, AR 72203

The purpose of *QEX* is to:

1) provide a medium for the exchange of ideas and information among Amateur Radio experimenters,

2) document advanced technical work in the Amateur Radio field, and

3) support efforts to advance the state of the Amateur Radio art.

All correspondence concerning *QEX* should be addressed to the American Radio Relay League, 225 Main St., Newington, CT 06111 USA. Envelopes containing manuscripts and letters for publication in *QEX* should be marked Editor, *QEX*.

Both theoretical and practical technical articles are welcomed. Manuscripts should be submitted in word-processor format, if possible. We can redraw any figures as long as their content is clear. Photos should be glossy, color or black-and-white prints of at least the size they are to appear in *QEX* or high-resolution digital images (300 dots per inch or higher at the printed size). Further information for authors can be found on the Web at **www.arrl.org/qex/** or by e-mail to **qex@arrl.org**.

Any opinions expressed in *QEX* are those of the authors, not necessarily those of the Editor or the League. While we strive to ensure all material is technically correct, authors are expected to defend their own assertions. Products mentioned are included for your information only; no endorsement is implied. Readers are cautioned to verify the availability of products before sending money to vendors.

Kazimierz "Kai" Siwiak, KE4PT

Perspectives

Re-cycling Electronics

During my early days in amateur radio — in the mid 1960s — my main source of electrical and electronics components for homebrewing ham gear was a discarded television chassis. After dismantling and sorting the components, there was almost enough to recycle a vacuum tube television set into a low-power ham transmitter — along with a healthy handful of resistors, capacitors and potentiometers to replenish the 'junk' box for other projects. I needed just a few additional specialized parts like crystals for frequency control. That was then. Today's discarded television sets do not yield many ham-salvageable components, which begs the question: "What can today's home brewer recycle into a ham project?"

Some discarded consumer items can still be recycled into ham gear. For example, a magnetron-based microwave oven can source the parts for a several hundred watt high-voltage power supply to breathe life into a home brew vacuum tube linear amplifier. The magnetron also yields a hefty refrigerator magnet.

I'd like to revisit this concept and publish an account of what you, dear reader and experimenter, have recycled into ham projects?

In This Issue:

- Tim Czerwonka, WO9U, creates custom keyboards using qmk firmware.
- Lynn Hansen, KU7Q, describes automation options for the CTR2 HMI.
- Chuck MacCluer, W8MQW, describes sequencing of antenna change-over relays.
- Eric Nichols, KL7AJ, in his Essay Series, describes angular frequency.
- Philip Cassady, K7PEC, reveals the effects height and ground parameters on a dipole.
- John Stanley, K4ERO, shows that loss on a line with SWR can be lower than on a matched line.
- Peter DeNeef, AE7PD, estimates the field power density from a parabolic dish antenna.
- Alan Victor, W4AMV, investigates transformer coupled tuned impedance transforming circuits.

Writing for *QEX*

Please continue to send in full-length *QEX* articles, or share a **Technical Note** of several hundred words in length plus a figure or two. *QEX* is edited by Kazimierz "Kai" Siwiak, KE4PT, (**ksiwiak@arrl.org**) and is published bimonthly. *QEX* is a forum for the free exchange of ideas among communications experimenters. All members can access digital editions of all four ARRL magazines: *QST*, *On the Air, QEX*, and *NCJ* as a member benefit. The *QEX printed edition* is available at an annual subscription rate (6 issues per year) for members and non-members, see **www.arrl.org/qex**.

Would you like to write for *QEX*? We pay $50 per published page for full articles and *QEX* Technical Notes. Get more information and an Author Guide at **www.arrl.org/qex-author-guide**. If you prefer postal mail, send a business-size self-addressed, stamped (US postage) envelope to: *QEX* Author Guide, c/o Maty Weinberg, ARRL, 225 Main St., Newington, CT 06111.

Very kindest regards,
Kazimierz "Kai" Siwiak, KE4PT
QEX Editor

Tim Czerwonka, WO9U

N8817 Badger Rd., Blanchardville, WI 53516; **tczerwonka@gmail.com**

Custom Keyboards with *qmk* Firmware

Simplify tasks in radio-related PC applications by creating custom PC keyboards.

This article describes using the open-source *qmk* firmware on an inexpensive microcontroller to create a custom PC keyboard that simplifies tasks in radio-related PC applications. PCs and software applications are important tools in the ham shack and home lab. Dedicated combinations of key presses, or hotkeys save time and simplify software operation. A custom keypad in addition to your normal keyboard can make accessing these hotkeys very convenient.

My goal was to build a separate PC keyboard with unique single-press key codes not normally available on a regular keyboard. For example a single key press for "shift+F12" could be programmed to be a useful keystroke in various ham radio programs. Additionally pre-populated text strings or a single keypress for characters such as "μ" is a convenience in the occasional email or other writing.

I am using an open-source microcontroller firmware called *qmk* (Quantum Mechanical Keyboard) **[1]** to create my own customized keyboard interface for key macros in software that I use frequently. It is an open-source community centered around developing computer input devices. The *qmk* firmware, when combined with one of several commonly available microcontrollers and an array of switches, allows a great deal of flexibility to automate key presses or mouse movements.

I built three interfaces with *qmk* firmware. The first is a simple rotary encoder with five programmable buttons and OLED display for use with my software-defined radio (**Figure 1 left**). The second is a commercial USB numeric keypad where I substituted my own microcontroller and firmware to achieve the desired programmability. The third (**Figure 1 right**) is an inexpensive 16-key macropad kit that would prove a quick and inexpensive keyboard addition in any ham shack, desktop or workbench.

Figure 1 — A rotary encoder (left), and 16 key encoder (right).

General Architecture

Keyboards are arrays of switches arranged in a matrix of rows and columns. The rows and columns are scanned by a microcontroller for switch closure upon which a key event is sent to the PC. For example, a matrix with four rows and four columns could support 16 keys. The four rows and four columns require connection

to eight pins on the microcontroller. Diodes are often used with the key switch matrix to prevent misreading if multiple keys are selected at the same time. The *qmk* firmware is set up with the desired microcontroller pin configuration, number of rows and columns, and the key codes to be sent to the host PC upon keypress. When programmed with the *qmk* firmware, the microcontroller presents itself as a USB-connected keyboard to the host computer.

A keyboard layer is an alternative character set to be sent upon keypress. A typical keyboard has several keys that affect key layers — such as when "shift" is pressed, the key that normally generates a lower-case letter will generate an upper-case letter. When you are in control of the firmware, your chosen "shift" key may toggle between one or many layers providing key or string combinations specific to a program or function. The layer change can be temporary upon keypress or rotate through multiple layers.

I am using the Pro Micro, an Arduino-compatible development board, which uses the Atmel ATMega32U4 microcontroller. This commonly available board has a native USB interface and enough I/O pins for many applications. All firmware programming is done using your PC's USB connection, which leads to easy experimentation and rapid development cycles when changes need to be made.

qmk Firmware

The *qmk* website has great step-by-step directions and explanations on how to download the firmware, flash a microcontroller and make custom key maps using a Windows, Macintosh or Linux platform. It also covers simple usage of the 'git' version control system **[2]** to allow you to make revision-controlled changes of your own against the main *qmk* firmware codebase. I opted to make a 'fork' of the *qmk* firmware in my own github account **[3]** to keep track of changes and additions necessary for my hardware. The *qmk* documentation includes information on maintaining your code revisions in github.

Keypad for SDR

I built an interface for use with my Flex-6300 SDR. The interface includes a large rotary encoder, five buttons and a small SSD1306 OLED display. To simplify firmware configuration, I chose to represent the five buttons as one column with five rows. One button toggles through several layers for different button functions customized for use with *SmartSDR*, *WSJT-X*, and *N1MM Logger*. I am using *DDUtilV3* **[4]** to map custom keypresses to *SmartSDR* functions. See **Table 1**.

The OLED display indicates which of the multiple layers are active and the function for each button. A rotary encoder is configured to send mouse wheel up and down events for SDR tuning. The rotary encoder I selected was found as a "CNC Hand Wheel Manual Pulse Encoder" on **amazon.com**. This knob has Gray code output with 100 pulses per revolution. As received from the manufacturer the knob also has 100 physical detents per revolution, a property I did not want in a tuning knob. To disable the detents, I removed the crank pin screw and carefully lifted the circular faceplate that is attached by double-sided adhesive tape. Removing the three screws underneath releases the knob. A thin metal plate retains the spring and pin arrangement providing the detent action. I discarded the spring and pin. I am confident this voids any warranty; you may wish to test your rotary encoder prior to modification. A sample list of ordered parts is found in **Table 2**. **Figure 2** shows a schematic for this hardware.

Note, unlike the *FlexControl* USB

Table 1 – One button toggles through several layers for different customized button functions

layer: BASE.

Action function	Key	DDUTIL
Mute	Shift + F9	SMUTEALL
Step Up	Shift + F16	STEPINC
Step Down	Shift + F17	STEPDEC
Task switch	alt+tab	

layer: MODE

Action function	*Key*	*DDUTIL*
Mute	Shift + F9	SMUTEALL
Mode Up	Shift + F14	SMODENEXT
Mode Down	Shift + F15	SMODEPREV
Task switch	alt+tab	

layer: ZOOM

Action function	*Key*	*DDUTIL*
Mute	Shift + F9	SMUTEALL
Pan Up	Shift + F19	PANBW_UP
Pan Down	Shift + F11	PANBW_ DOWN
Pan Center	Shift + F13	PANCENTER

layer: WSJT

Action	*Key*
Muste	Shift + F9
Enable TX	Alt + N
Erase	Alt + E
Halt TX	Alt + H

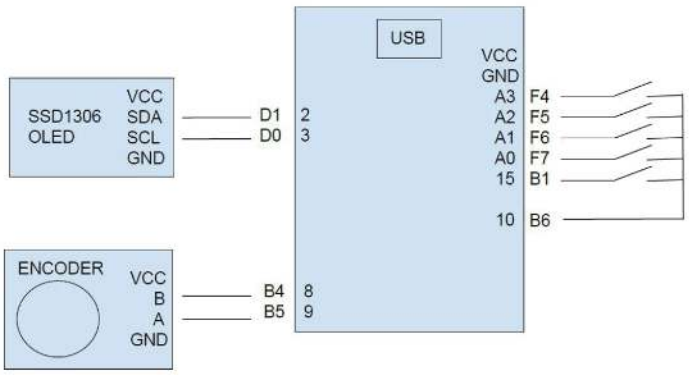

Figure 2 — Schematic for the hardware.

Table 2 – Sample parts list from amazon.com, provided as a reference to assist with selecting components from a vendor of choice.

Amazon ASIN	*Description*
B08BJNV1J3	Pro Micro Atmega32U4 5V microcontroller
B08LYL7QFQ	0.96 Inch OLED Module 12864 128x64 SSD1306
B07Q75KT49	6 Terminal Manual Pulse Encoder

knob, this mouse wheel tuning function does not function unless the main window of *SmartSDR* is in focus. For my purposes this caveat isn't problematic and I find this method of tuning very convenient.

The code I used to define this tuning knob and keypad is located here:
https://github.com/tczerwonka/qmk_firmware/tree/master/keyboards/tczerwonka_rotary

To build and flash this code to my microcontroller I would issue the following command on my Linux desktop where I have previously configured the *qmk* build environment:

```
make tczerwonka
rotary:sdrknob:avrdude
```

If your build is successful, reset the microcontroller when prompted. Changes specific to your station can be made in your local copy of the code and tested quickly.

Modify Existing Keyboard

I have an older commercially produced numeric keypad excess to my needs. Could I use this with *qmk* firmware? The original on-board microcontroller is of an unknown type and likely one-time programmed by the manufacturer. I disassembled the keypad and made notes on how the keypad's manufacturer routed the rows and columns on the keypad's flexible printed circuit (FPC) switch matrix. I then cut the traces between the original circuit board's flexible flat cable (FFC) connectors and the original microprocessor, soldering in short wires from the FFC connectors to my Pro Micro board. For the *qmk* firmware I created a new subdirectory in my github *qmk* firmware repository specific for this keypad and added configuration to support my new keyboard and desired layout. As there were several unused pins on my microcontroller I added four LEDs on the keypad to indicate the keypad's active layer. The process of determining my keypad's existing matrix and expressing it in code involved some trial and error but it went quickly as an iterative build / flash / test / modify development process can be completed in well under a minute. This was a fun one-evening junk box-sourced project.

Figure 3 — The components of a 1UP Keyboard kit.

1UP Keyboards Macropad

There are multiple commercial sources for full keyboards and small macropads which use the *qmk* firmware. I purchased an inexpensive sixteen key macropad kit from 1UP keyboards **[5]**, which consists of a PC board, sixteen mechanical keys, keycaps, microcontroller and other necessary parts (**Figure 3**). Many options for mechanical keys are available, each with varying degrees of click, stiffness and travel. Assembly was quick and programming with the default firmware was simple. The *1UP Keyboard* firmware is available in the *qmk* firmware github repository.

I chose to have this keyboard contain the same functions as my SDR interface in addition to having an array of common symbols. My keypad configuration contains additional layers for use not only with my ham applications but macros I use frequently at work. A macropad of this type would be an inexpensive and easily-built addition for many radio enthusiasts. My code is located at the following location; it should be easy to modify as necessary for your own requirements.

https://github.com/tczerwonka/qmk_firmware/tree/master/keyboards/1upkeyboards/sweet16/keymaps/tczerwonka

In conclusion, the *qmk* firmware offers a simple firmware platform to generate key combinations with your custom hardware that has the potential to simplify many software or radio tasks.

[Photos by the author].

Tim Czerwonka, WO9U, became a ham in 1989 at age 14. He has a BS in atmospheric and oceanic sciences from the University of Wisconsin – Madison. Tim is currently a network engineer for UW – Madison with an interest in monitoring and forecasting.

References

[1] **https://docs.qmk.fm/**
[2] **https://git-scm.com/**
[3] **https://github.com/tczerwonka**
[4] **k5fr.com/DDUtilV3wiki/**
[5] **https://www.1upkeyboards.com/**

Lynn H. Hansen, KU7Q

10914 Westchester Dr., P.O. Box 301, Lava Hot Springs, ID 83246; **lynn@lynovation.com**

Automation Options for the CTR2 HMI

This comprehensive station control system supports several switching options that can be added at any time and in any order.

The September/October 2021 issue of *QEX* presented Control the Radio 2 (CTR2), a multi-radio Human-Machine-Interface (HMI) capable of controlling multiple radios. At each radio, an I/O module collects audio, CAT control, and keying signals and transports them to the HMI using CAT5 cable. In its simplest form a single radio I/O module connects directly to the HMI. The system can be expanded using manual RJ45 switches (not Ethernet switches) to connect any number of radios to the HMI.

Routing radio I/O to the HMI is only part of the challenge when controlling multiple radios. The antenna distribution system must also be considered. Antenna selection and routing to the operating radio can be done using a patch panel or manual antenna switches. As the number of radios and antennas increases these methods quickly become cumbersome.

To fully realize a comprehensive station control system, three switching options are supported by the CTR2 HMI. These options can be added individually at any time and in any order. This allows you to build the station controller to suit your needs today and in the future.

Switching options include:

• An ASC (Antenna Switch Controller) and it's associated remote antenna switch to route up to 8 antennas in any combination to a common antenna port.

• An RASC (Radio Antenna Switch Controller) together with up to two 8-port remote antenna switches route the common antenna port from the ASC switch to one of sixteen radios.

• An RJ45 switch that synchronizes with the RASC to route the selected radio's audio, CAT, and key control to the HMI.

Both antenna switch controllers are designed to control either a homebrew remote switch like the 8-channel remote control antenna selector presented by Michael Dzado, ACØHB, in the March/April 2014 issue of *QEX*, or a commercial antenna switch such as the DX Engineering RR8B-HP. See the **Sidebar – Antenna Switches**. Options are provided to source +12 V dc, sink ground, or use an external power source to control the switches of your choice.

Antenna Switches

A word about antenna switches.

When it comes to switching a common antenna between two or more radios, go for the most isolation you can afford. Dzado's March/April 2014 *QEX*, article goes into great detail on what it takes to design a proper antenna switch with high port isolation. If you run at legal power limits you'll need a minimum of 70 dB isolation. 60 dB is sufficient for 100 W. Resist the temptation to buy inexpensive antenna switches from internet merchants, especially if they don't list or guarantee the port isolation of their switch. Many inexpensive switches have less than 30 dB of isolation. Excessive RF coupling can easily damage your expensive offline receivers. Isolation requirements are not quite as critical for switching multiple antennas. However, using an antenna switch with low port isolation here will degrade your antenna system's performance.

CTR2 System Build-Out

Figure 1 shows the functional drawing of a fully built-out CTR2 system using the automated switches described in this article. The antenna switch routes one or more of the available antennas to a common port. This switch is controlled by the CTR2 ASC. The switch itself is usually mounted outside, and the 9-wire shielded control cable and common antenna coax run back to the station. Once in the station, the coax can be connected to an optional antenna tuner then to the common port of one or two 8-port radio antenna switches under control of the CTR2 RASC. Individual coax runs from these switches then feed each radio.

The RJ45 switch consists of one to four 4-port RJ45 switch boards. The RASC and the RJ45 switch work together to route the antenna to the selected radio and the I/O from that radio to the HMI. The ASC works independently and can be configured in the HMI to switch antennas based on radio and band selection. It also allows two or more antennas to be selected at the same time if you use phased arrays.

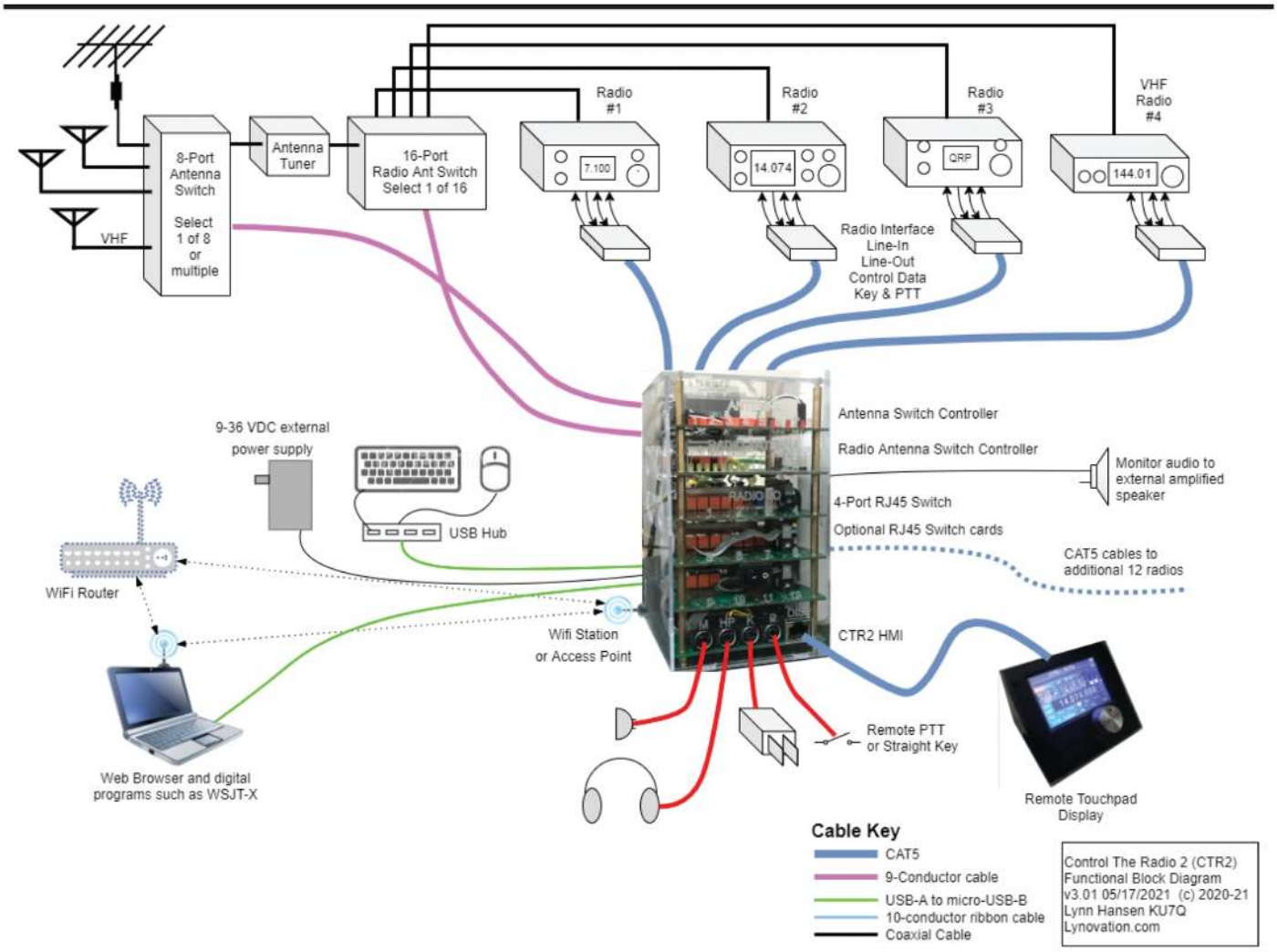

Figure 1 — Functional drawing of the fully built-out CTR2 system.

Logic Circuit Description

The same basic logic circuit is used for all three switch controllers. Referring to the logic section schematic, **Figure 2**, the heart of the circuit is IC1, a CD4514 CMOS 4-Bit Latch/4-to-16 Line Decoder chip. This chip takes a 4-bit address (Data 1, 2, 3, and 4) and decodes the binary value to drive one of 16 outputs. A **STROBE** signal is driven **HIGH** to **LOW** to latch the address into the decoder. Once this is done the **INHIBIT** signal is driven **LOW** to force the selected output pin **HIGH**. Low pass filters are installed on all signal lines for RF isolation.

The output pins of the CD4514 decoder are routed to two ULN2803 Darlington transistor arrays, IC2 and IC3. These devices each provide 8 Darlington transistor pairs and are designed to drive relays and stepper motors from TTL or CMOS inputs. They can sink up to 50 V at 500 mA and have integrated clamping diodes to shunt the inductive kickback when operating inductive loads such as relays. They are inverters so, a **HIGH** input level causes the output to go **LOW**.

Full schematics and bill of materials for each board can be found on my web site, **https://ctr2.lynovation.com/**.

Antenna Switch Controller (ASC) Circuit Description

The CTR2 ASC operates independently from the other two switches in that it can select up to 8 relays in any combination. To do this, 12 V latching relays are employed.

To operate a relay the HMI sends a **SET** or **RESET** address to U1. Addresses 0 to 7 operate the **SET** relay in K1 to K8 and addresses 8 to 15 operate the **RESET** relay in K1 to K8. Power to the coil can be removed once the position is latched into the relay.

On U1 the **INHIBIT** input is connected to the **STROBE** input through an RC delay circuit. The **STROBE** and **INHIBIT** inputs are normally kept **HIGH**, disabling all outputs. To operate a relay its address is asserted on the **DATA** lines then the **STROBE/INHIBIT** line is driven **LOW** to latch the address and drive the selected output of U1 **HIGH**. The Darlington driver output on U2 or U3 then goes **LOW** which latches the selected state (**SET** or **RESET**) in the relay. After 10 ms the **STROBE/INHIBIT** is driven **HIGH** again disabling all outputs from U1 and deactivating the selected relay coil. A small time delay RC network (R9 and C22) delays the **INHIBIT** signal for a short time to allow the decoder time to decode the address.

The **Antenna Selection** page, **Figure 3**, in the HMI visually displays the antenna switch configuration and controls the ASC. There are options to allow single or multiple antenna selections, select antennas based on the selected band, tag each antenna with a name, and reset all settings back to default.

The **[Save]** button saves new settings to the radio's database.

TB1 is used to connect the ASC to the antenna switch. Both +12 V dc and ground are available on this terminal block to provide the required return path. A 9-conductor wire is needed to control the 8 relays on the switch. MOVs are provided to suppress any induced voltages from the field since the switch will generally be mounted outside.

There are several options to provide power to the ASC and RASC boards and their associated remote switches. These options are described on the Lynovation web site.

Radio Antenna Switch Controller (RASC) Circuit Description

The RASC operates in sync with the RJ45 switch. Its job is to control up to two 8-port remote antenna switches to route the common antenna port from the ASC controlled antenna switch to one of 16 radios.

This board uses the same addressing logic as the ASC with the exception that the **STROBE** and **INHIBIT** inputs to U1 are controlled separately and momentary relays are used. Once one of the 16 relays is selected, the **INHIBIT** input is pulled **LOW** to keep the selected relay activated. This ensures that one, and only one, relay can be active at a time.

TB1 and TB2 are used to connect the antenna switches. TB1 controls switches 1 to 8. TB2 controls switches 9 to 16. Both +12 V dc and ground are available on these terminal blocks. MOVs are not provided on this controller since these antenna switches will generally be located inside near the radios.

Like the ACS, this board has multiple options to provide power to the external antenna switches.

RJ45 Switch Circuit Description

Figure 4 is a block diagram of the 16-port RJ45 switch. The system is comprised of a main switch board and up to three expansion boards. **Figure 5** is a close-up of the main switch board.

The main switch board interfaces to the HMI with two 10-conductor ribbon cables that connect to the RJ45 Switch Control and Radio I/O ports on the HMI. The main switch board routes radio I/O for ports 1 through 4. Additional 4-port expansion boards can be added to the system by connecting the Expansion Port (J3) on each expansion card to the 'Ports xx-xx' connector (J4, J5, or J6) on the main board and daisy-chaining the Radio I/O port to each board.

Decoding logic is the same as used on the RASC board. The Darlington drivers control four DPDT relays for each port. These relays route the eight wires from the HMI's Radio I/O port to the selected RJ45 port on the rear of the board. DPDT relays were chosen over 4PDT or 8PDT relays solely based on cost. Four DPDT relays cost around $7.00 while 4PDT and 8PDT relays are priced in the hundreds of dollars. Additionally, relays were chosen over

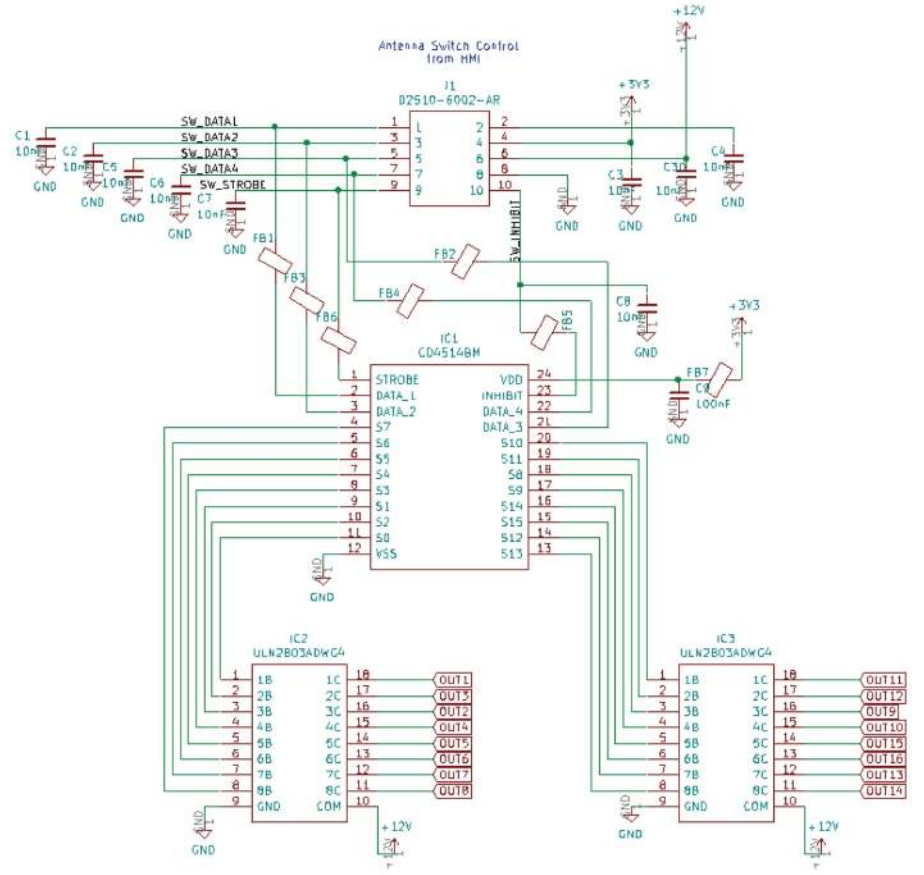

Figure 2 — Decoding logic circuit common to all switches.

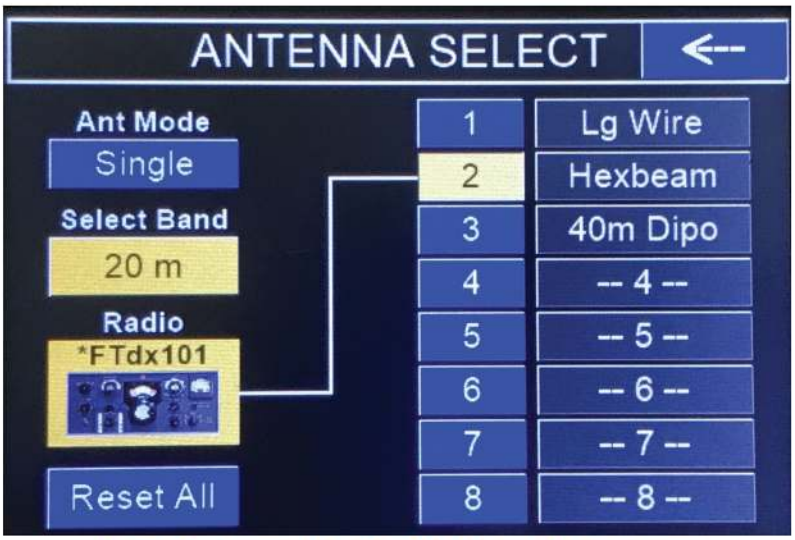

Figure 3 — Screen shot of the HMI Antenna Selection page.

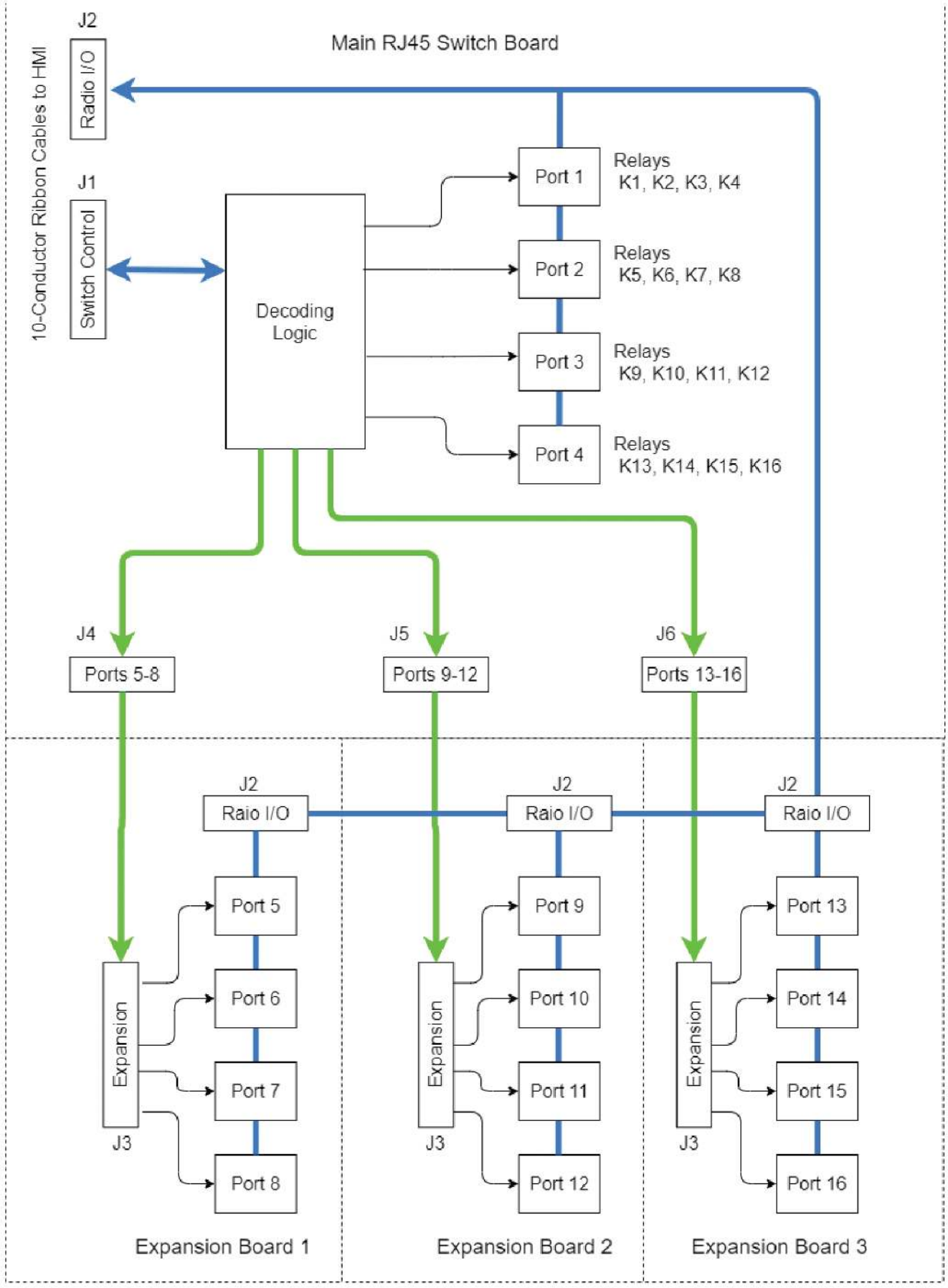

Figure 4 — Block diagram of the 16-port RJ45 switch.

solid-state switches or digital multiplexing because of cost and simplicity.

The data lines that drive the decoder are bi-directional and are also used to detect installed boards. This allows the HMI to "know" which expansion boards are installed. Sensing resistor R6 is connected to Data 1 and always pulls this line low (2.2 kΩ to ground) when it's not being used to set the decoder. Sensing resistors R5, R4, and R3 connect to Data 2, Data 3, and Data 4 respectively, and are pulled low when expansion boards 1, 2 or 3 are installed. To detect the installed boards the CPU momentarily switches the switch address output lines to input mode with "weak" pull-ups (around 20 kΩ to 3.3 V) then reads the values on these lines. Inputs connected to installed boards will be read as **LOW** when sampled.

The +5 V dc power is supplied by the CTR2 HMI and 5 V momentary relays are used throughout. A +3.3 V dc regulator on the main switch board provides power for the decoding logic.

Optional continuous or offline receiver monitoring for one radio on each board is provided for in this design. J10, J11, J12, and J13 tap both continuous and offline Rx audio from the four radio I/O interfaces. Pins 1-2 provide continuous Rx audio and pins 2-3 only sample Rx audio when the radio is offline (not selected in the HMI). Pins 1-2 or 2-3 are then connected to J8, the input of isolation transformer T1. A 3.5 mm phone jack can be connected to J9, the output of T1, to provide a connection to an external amplified speaker for monitoring Rx audio from this radio. Note that the monitored receiver must be connected to a separate antenna. I use this option with a PCR1000 wideband receiver to monitor activity on other bands.

Let's Build It

PCBs are required to build these boards because the connectors are not perf-board friendly. PCBs with all the SMD components pre-installed are available at **https://ctr2.lynovation.com/**.

Automated Bill of Material (BOM) files, as described in the September / October *QEX* article, are available for each board in the CTR2 series at my Lynovation web site. These files run in your browser and list the part numbers and dynamically show the part placement as you click on each part.

The RJ45 switch main and expansion boards are built using the same PCB. The main board requires all parts except the

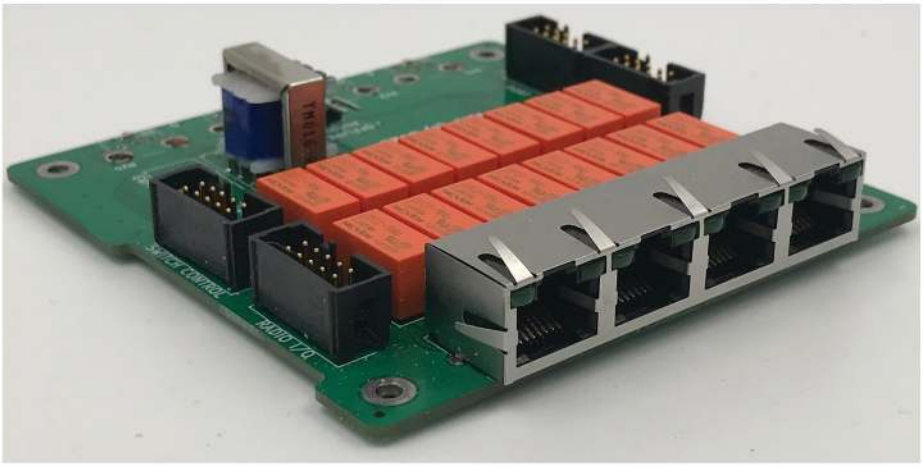

Figure 5 — Close-up of the main 4-port RJ45 switch board.

Figure 6 — CTR2 stack with HMI, three RJ45 switch boards, the ASC and the RASC.

Expansion Port (J3) to be installed. You can also leave off connectors for J4, J5, and/or J6 if you're not going to use those expansion boards. The Rx Audio monitor hardware is optional.

On the RJ45 expansion boards, install Expansion Port J3, the 16 relays, the 4-port RJ45 jack, LEDs D2 to D5, LED current limiting resistors R7 to R14, and RF bypass capacitors C9 to C12.

Let's Package It

As seen in **Figure 6,** CTR2 option boards are designed to stack on the HMI board. Start the stack using M3 6 mm male/female threaded standoffs on the bottom of the HMI board then add four M3 25 mm for each board, screwing each standoff into the one below the board. Each board adds 26.6 mm (a little over 1") to the stack so the HMI with four 4-port RJ45 switch board, an ASC and an RASC forms a stack 110 mm (approximately 4.25") square and 204 mm (8") high.

The assembly is self-supporting and can be left "open-frame" if you prefer. It can stand vertically or horizontally to fit your needs. If you have access to a CNC mill you can cut an interlocking enclosure for it from the dimensions supplied in the documentation on my web page. I can supply a limited number of pre-cut acrylic enclosures for this project. A 3D-printed enclosure is certainly possible but I haven't explored that option.

All boards connect to the HMI using 10-conductor ribbon cable and IDC connectors. Be sure to verify pin 1 is correctly oriented on each end of the cable and the cable is long enough *after you fold the cable back through the strain relief clamp* before you crimp the connector! There is a small arrow on the #1 pin side of the connector for reference as shown in **Figure 7**.

The Radio I/O cable will require additional connectors installed "mid-stream" if using RJ45 expansion boards. A 16 port switch requires 5 connectors on this cable. Space each connector so the finished distance between connectors is about 40 mm. I recommend purchasing extra IDC connectors and ribbon cable as they are easily broken or misaligned during installation. The cable must be precisely aligned in the connector before squeezing it together. A misaligned cable can cause short-circuits between the wires. Expansion pliers or a vise can be used to squeeze the connectors onto the ribbon cable, but an IDC installation tool makes the job much easier. Once the connector has been set, fold the ribbon cable over the top and install the strain relief clip. Before using them it's a good idea to check the continuity on each pin and verify that they are not shorted to adjacent pins.

Using the CTR2 System

Connect the CAT5 cables from the radio I/O modules to the RJ45 jacks on the back of the RJ45 switch, taking note of which radio is on each port. Power up the HMI and it will select the last radio port used. The LED of the active port on the front of the RJ45 switch lights as will the green LED on the active RJ45 connector on the back. If using the RASC the same # LED will light on it showing the common antenna port is connected to that radio. If using the ASC, the LED (or LEDs if more than one antenna is selected), will also light. If you are using CAT control, change the frequency on the HMI and verify the correct radio responds. On the HMI's **Home** page, **Figure 8** the **[R3:A2]** button indicates that radio #3 and antenna #2 are selected. Touch this button to open the **Radio Select** page, **Figure 9**. The selected port is highlighted in orange. If you have one or more expansion boards installed, as in this case, the background surrounding their ports will be orange also. In this example the main switch board and

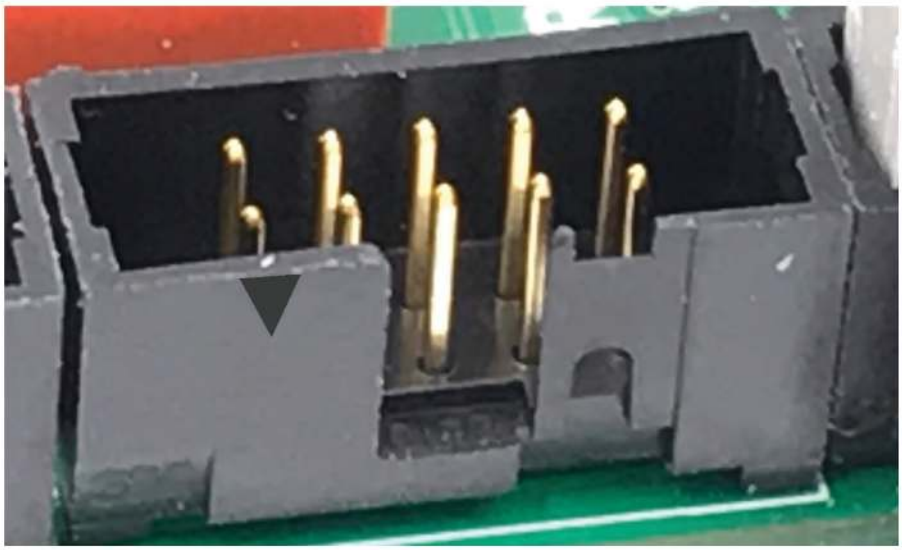

Figure 7 — Close up of the #1 pin mark on the 10-pin IDC connector.

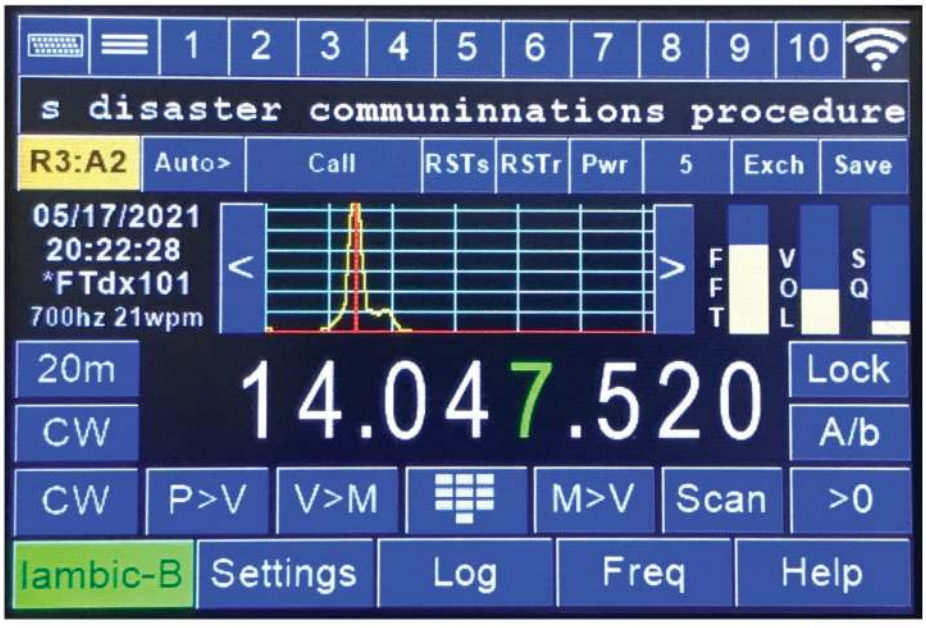

Figure 8 — Screen shot of the HMI Home page.

one 4-port extension board is installed and Port 3 is selected (my FTdx101). To select another radio just touch the numbered blue button below its caption.

To edit the caption for each port touch the black area above the numbered blue select button. This caption will be displayed on the **Home** page just below the date and time. It is also displayed when loading the radio files and when connecting to the HMI via its web server. On the **Radio Select** page you can also copy or erase a port's settings.

• Touch **[Copy]** then select one of the other ports to copy the current settings to.

• Touch **[Erase]** to erase the currently selected port.

Ports can share a common database by touching the **[SharedDB]** button. This allows every radio sharing the common database to have the same favorite frequency list, transmit buffers, band registers, and antenna settings. Changes made while the common database is selected will appear on all of the radios sharing this database. The **[R#:A#]** button on the **Home** page will be red when the common database is selected and orange when it is not.

To select antennas, touch the **[R#:A#]** or **[Band]** button on the **Home** page then touch the **[Set Ant]** button at the top of the page. The **Antenna Selection** page will open **Figure 3**. The default is to assign a single antenna for all bands. Touching the **[Band Select]** button takes you to the **Band** page **Figure 10**. This page shows the assigned antenna for each band in the small black box on each button. Selecting a band here returns you to the **[Set Ant]** page where you select the antenna for it. Continue this back and forth process until all bands have been mapped to an antenna. The HMI will now automatically switch to the selected antenna as you change bands. These settings are saved in the radio's database or the common database if you have **[ShareDB]** selected.

Figure 9 — Screen shot of the HMI Radio Select page.

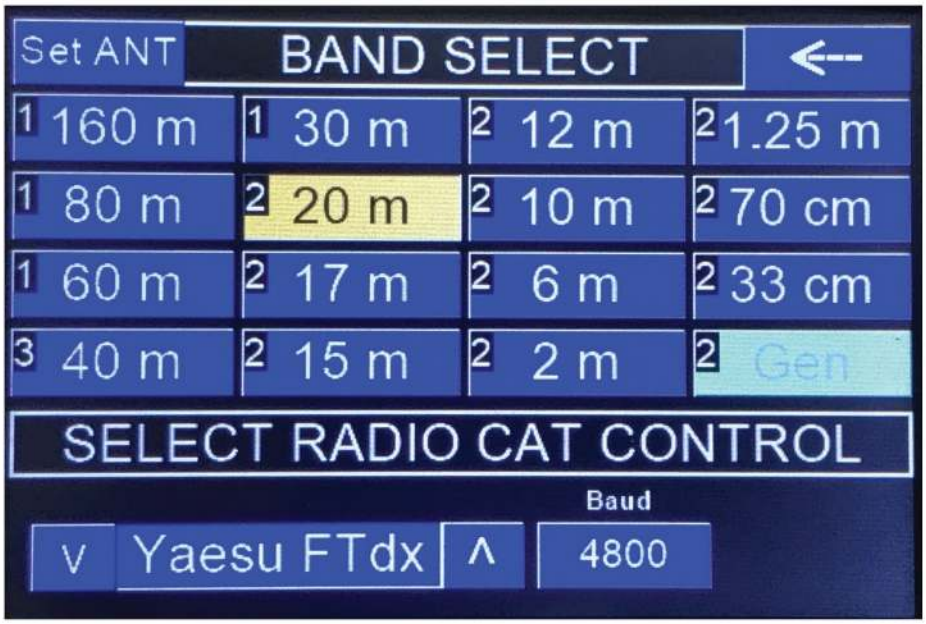

Figure 10 — Screen shot of the HMI Band page.

Wrapping It Up

You might be wondering if there is a real need for such a switching mechanism when it's relatively easy to just move your headphones, paddles, mic, remote PTT switch, antenna, and PC to the radio you want to operate. After all, you've probably been doing that for years. This is especially true if you rarely operate multiple radios. In my case I have acquired many radios during the years I've spent in this hobby and plan on acquiring a few more! I tend to keep my radios instead of selling them to buy the next flavor of the month and I still enjoy using the old ones on occasion. But technology has spoiled me. I like a lot of the features in the new radios like touch tuning, voice keying, etc., and decided to create a system that provides as many of these features as possible for my older radios.

Is CTR2 and its automation options overkill? Sure it is. But for me it's part of the fun of ham radio. It might not be for you and that's okay. I do hope that you have found something useful or inspiring in these projects. For me, DSP is no longer in the realm of magic. The **PJRC.com** Teensy ecosystem has placed DSP in the hands of us mere mortals. Use your imagination and learn how to create something that works for you.

If you manage a club station you might consider building a station controller as a club project. CTR2 board assemblies can be constructed by club members with varying skill levels. The HMI board requires the most skill whereas the switch boards are mostly mounting relays and connectors. Since every club has one or more software gurus, let them customize the HMI software

to fit your needs.

The latest updates on this project including firmware, source code, and PCB/enclosure ordering information can be found on my website, **https://ctr2.lynovation.com/**. I'll also be posting features and how-to videos to my YouTube channel. Search for Lynovation.

[Photos by the author].

ARRL member Lynn Hansen, KU7Q, was first licensed in 1971 as WN7QYG at the age of 14. He achieved the Amateur Extra class level and became KU7Q in 1981 while studying for his Commercial Radio Telephone license. His amateur radio experience, several Cleveland Institute of Electronics (CIE) home-study courses, and an innate desire to learn something new every day provided a career in electronics and communications as a utility communications technician, an engineering assistant, and finally as the operations manager over a large multi-state utility communications network. Now retired, he continues to learn and apply new technologies and has time to follow his passions. This project is one of many.

Errata

QEX Nov./Dec. 2021

In George R. Steber, WB9LVI, "*NanoSSB RX – An Ultra Low Cost SSB Multiband Receiver,*" *QEX* Nov./Dec. 2021, **Figure 3**, each of the two boxes to the right of the DSP should be labeled "DAC." Thanks to Wes Plouff, AC8JF, who spotted the error.

QEX Sep./Oct. 2021

In Luiz Duarte Lopes, CT1EOJ, "*Designing an Impedance Matching Network with a Drafting Ruler and Triangle,*" *QEX* Sep./Oct. 2021, the vector **BE** in **Figure 3** lags the vector **AD**, so it is an inductor. The vector **FD** should be **DF** with the arrow pointing to **F**. This component is a capacitor. In **Figure 2** reverse the position of the components *C* and *L*. In the *Final Calculations*,

$$X_L = V_a / I_L = 122.5 / 3.62 = 33.84$$

$$X_C = V_C / I_0 = 100 / 1.414 = 70.72$$

$$L = \frac{X_L}{2\pi f} = \frac{33.84}{2\pi \times 14.215} = 0.38\ \mu\text{H}$$

$$C = \frac{1}{2\pi f X_C} = \frac{10^6}{2\pi \times 14.215 \times 70.72} = 158\ \text{pF}.$$

Finally, delete **Figure 4** and delete the section *Confirmation* and everything under it, including **Table 1**, except the last paragraph. Thanks to Frank Fusari, W8KA, who called attention to the problem.

QEX Jan./Feb. 2021

In Eric P. Nichols, KL7AJ, "*Self-Paced Essays — #3 EE Math the Easy Way,*" *QEX* Sep./Oct. 2021, p. 19, we should have referred to Beverly Dudley as Mr. Dudley. We regret the error. Thanks to Richard Clark, WQ9T, who called attention to the problem.

QEX Jul./Aug. 2016

In Gene Hinkle, K5PA, "*Radio Frequency (RF) Surge Suppressor Ratings for Transmissions into Reactive Loads*," *QEX* Jul./Aug. 2016, the missing reference is:

[8] *The Antenna Handbook*, 23rd Edition, pp. 23-13, [Eq. 18].

Thanks to Mike Zydiak, W2MJZ, for calling the omission to our attention.

Chuck MacCluer, W8MQW

1390 E. Haslett Rd., Williamston, MI 48895; **w8mqw@arrl.net**

Amplifier Sequencing and Other Relay Pathologies

Mechanical rebound and sliding surface contacts can result in bad behavior of antenna changeover relays.

Hot switching can be catastrophic for relays and for the amplifiers that they are serving. RF should not be applied before a relay has completely closed, nor should RF be flowing as a relay opens. The antenna changeover relays used in high power amplifiers must be carefully sequenced to prevent such hot switching. Examine a snapshot of the act of closing a typical sealed antenna relay in **Figure 1**. Note the 1 ms of faulty conduction before the relay finally settles. The sequence timing of the changeover should allow for this transient delay in settling.

Even more disturbing, note the return-spring induced bounce as the relay returns to its normally closed position as shown in **Figure 2**. In this case elastic bounce totally interrupts the conductive path for over 1 ms. Fortunately, this bounce is harmless in antenna change-over circuits since only miniscule receive currents are being conducted. The sole exception is in VHF/UHF work where delicate mast-mounted preamplifiers are commonly protected by designing so that transmitting takes place in the normally closed position.

Proper Amplifier Sequencing

Figure 3 shows a typical amplifier changeover relay circuit. It involves three SPDT relays. The first, K1, switches the antenna from a receive common to the output of the amplifier. The second, K2, switches the transceiver from the receive common to the amplifier input. The third, K3, turns on the operating bias (or completes the cathode return) to the amplifier.

In its most rudimentary form in entry-level amplifiers, K1, K2, and K3 are the three poles of a single TPDT relay, where the armature of K3 has been carefully bent to produce safe sequencing **[1]**. Often, K1 and K2 are switched simultaneously. The crucial issue is the timing of K3 relative to K1 and K2. This is well travelled ground, see **[1]**, **[2]**, and **[3]**.

In summary, amplifier bias must not be applied until the transmit path is closed and bias must be removed before the transmit path is opened. We assume that our modern transceiver is itself properly

Figure 1 — A sealed relay closes 7 ms after 12 V is applied to its solenoid coil. The 12 V on the moving armature appears at its normally-open port followed by 1 ms of transient noise from mechanical rebound and sliding surface contact.

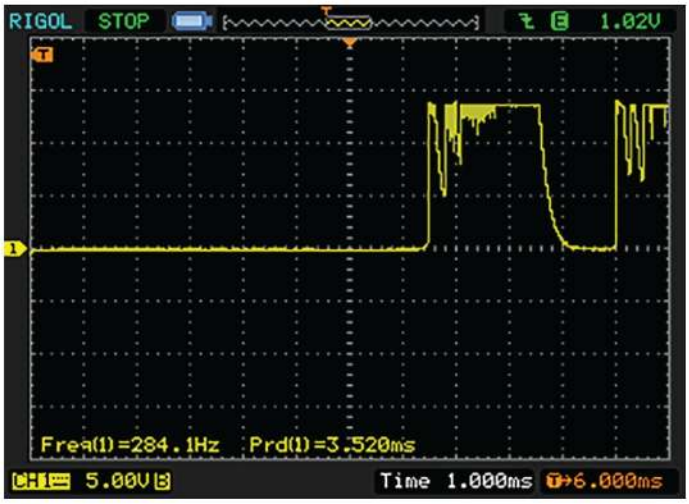

Figure 2 — The relay is de-energized and returns to its normally closed position. But unlike the electrically induced make, the return is induced mechanically by a coiled spring, producing a severe 1.25 ms bounce that completely severs conduction.

sequenced, allowing time for the amplifier changeover to settle before RF is present. For legacy transceivers, a more extensive, external sequencer must be used that properly sequences both the transceiver and the amplifier.

Some Traditional Sequencing Circuit Designs

An old standby sequencer design is a simplified version of the charging capacitor, stacked comparators used for VHF/UHF transverter sequencing **[4]** and **[5]**. The thresholds of a stacked series of comparator/relay drivers are indexed by a voltage divider, while all comparators sense the voltage across a charging capacitor. As the capacitor voltage rises, each comparator's threshold is reached in ascending order, closing its associated relay. When the PTT is released, the capacitor voltage falls and each comparator shuts down in turn once its threshold is passed.

More recently, sequencers have been implemented by an inexpensive CPU (e.g., Arduino, ATtiny, etc.) controlling relay drivers **[5]**, **[6]** and **[7]**. Here a looping routine waits for a change in the status of PTT. If a change occurs, the new status is read and the relay system spools up or down depending upon the status. The designer has complete control of each timing interval by changing a single number in one line of code.

For decades Ameritron has used the sequencer circuit of **Figure 4** in many of their vacuum tube amplifiers **[2]**. A 12 V ac transformer winding is used for a voltage doubler that supplies 24 V dc to the changeover board, while a midpoint capacitor tap supplies 12 V dc housekeeping voltage for the rest of the amplifier. The changeover board employs two identical DPDT 12 V Potter & Brumfield sealed relays, where the contacts of the first, K1, are doubled to carry the higher RF output current, and where the second relay makes up K2 and K3. The applied transient 24 V is used to initially overvoltage K1 in order to shorten its closure time. The closure of K2/K3 is delayed by a charging electrolytic capacitor. Upon PTT release, K1 is held closed for a time by the currents repeatedly circulating through its coil via its shunt reverse diode.

A disadvantage of this design is that the transceiver's open collector/drain PTT switch must carry relay onset currents and transients. Moreover, truly frightful voltages can appear at the collector of the top NPN transistor of **Figure 4** as the PTT is released. **Figure 5** shows a sample of the voltage waveforms that can occur at the bottom of the coil of K2/K3. In this case there are many short spikes of 60 V and voltages as high as 90 V! A reverse protection diode is ruled out in the Ameritron design by timing requirements.

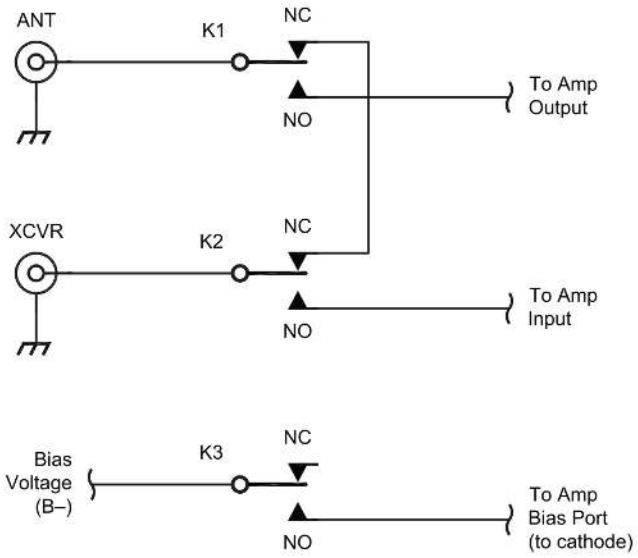

Figure 3 — This antenna changeover circuit is used universally in amplifiers not switched by PIN diodes. K1 is closed first followed by K2, Often they are simultaneously closed. K3 must be carefully sequenced to avoid hot switching.

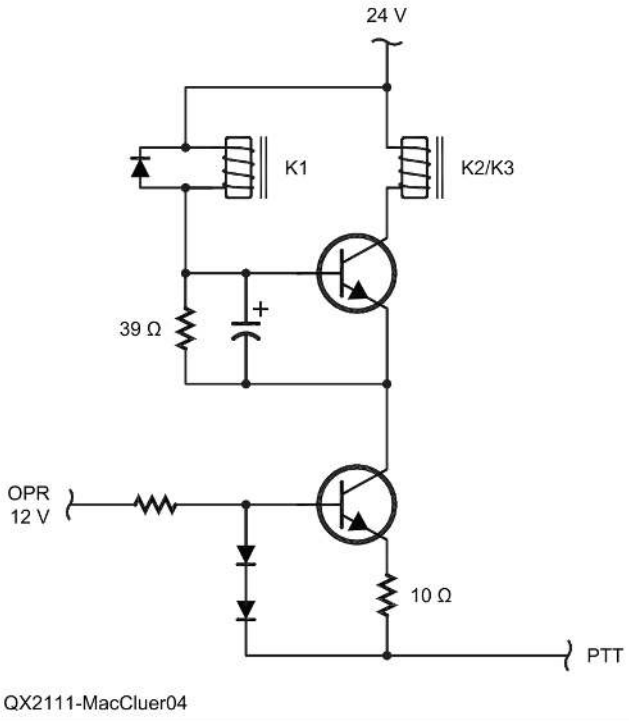

Figure 4 — A sketch of the Ameritron sequencer used in their larger vacuum tube amplifiers.

A Simple Alternate Design

Another approach exploits the inherent properties of the relays themselves. **Figure 6** shows an evolution of the Ameritron design

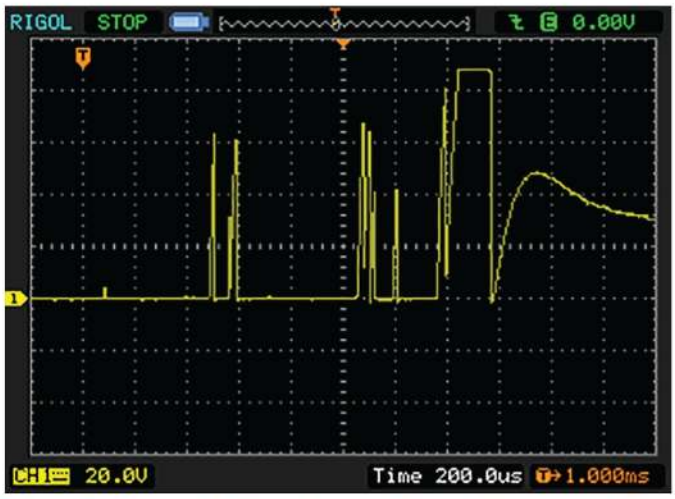

Figure 5 — A sample of the extreme voltages that can occur at the bottom of K2/K3 coil when PTT is released.

using three robust, inexpensive sealed Tianbo relays rather than the smaller Potter & Brumfield relays employed by Ameritron. This design can be used to replace the changeover board in older Ameritron amplifiers or in a new build.

Sequencing is obtained simply by the 100 Ω resistor in series with the coil of K3. Although the Tip32A power PNP transistor simultaneously provides a path for current to all three relay coils, the K3 series resistor delays its closing by 2.5 ms. Upon release of the PTT when the PNP transistor opens, the stored inductive energy delays the release of the relay contacts as currents repeatedly circulate and dissipate through each coil via the reverse shunt diode. However, relatively more power is dissipated by the 100 Ω series resistor, thus allowing K3 to release 1 ms sooner than K1 and K2. Here "release" is when the armature breaks contact with the

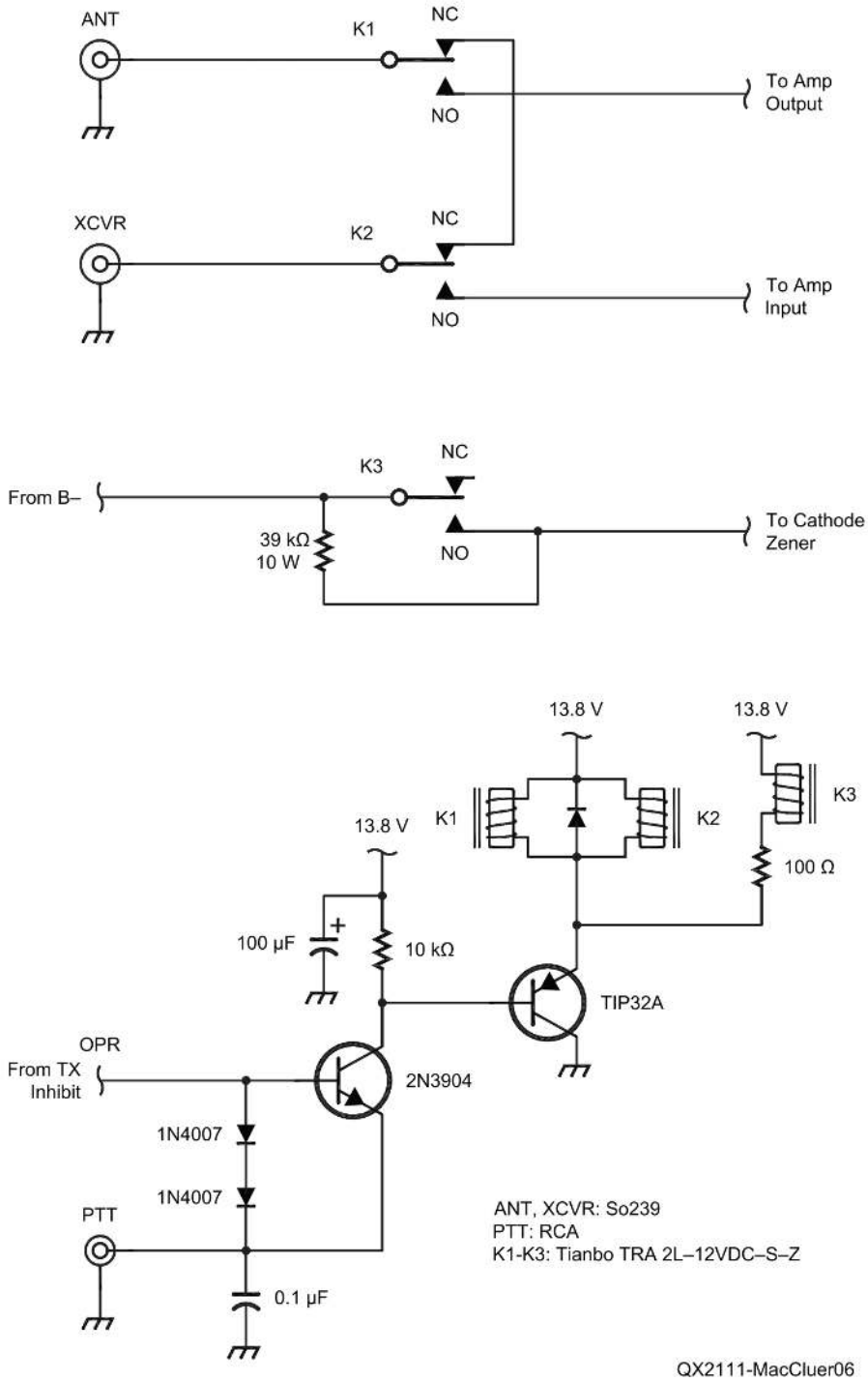

Figure 6 — A replacement for the Ameritron changeover board uses three identical Tianbo relays. The Tip32A power PNP transistor provides the current for all three relays. The series 100 Ω resistor delays the closing of K3 but speeds its release by consuming more circulating currents.

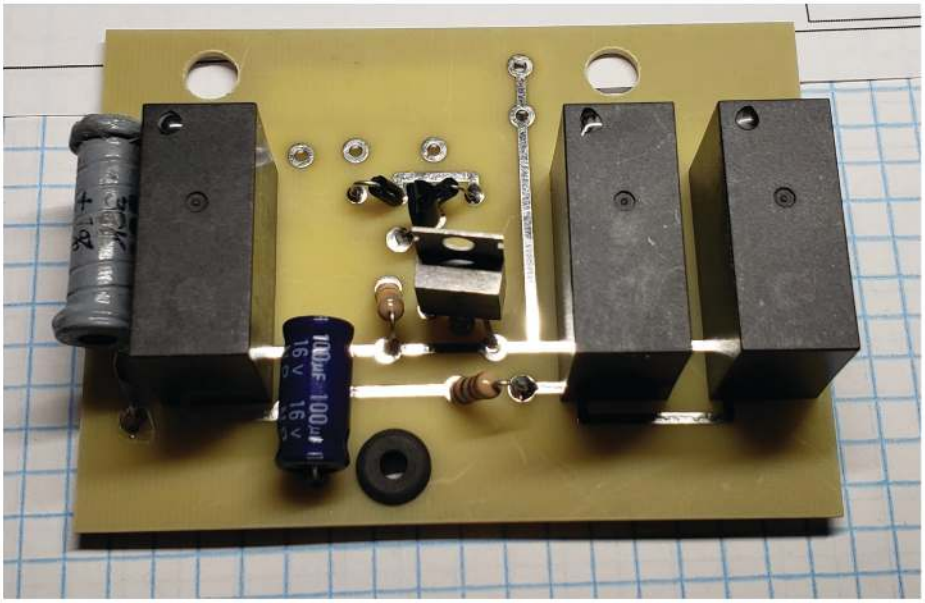

Figure 7 — The completed changeover board of Figure 6. [Photo by the author.]

normally open (NO) poles and "return" is when the armature returns to its normally closed (NC) position. The observed timing is as follows:

- K1 and K2 make in 8 ms,
- K3 makes in 10.5 ms,
- K1 and K2 release in 6 ms,
- K3 releases in 5 ms,
- K1 and K2 return in 7.25 ms.

The return of K3 is irrelevant.

In contrast to the Ameritron board, the transceiver's open collector/drain PTT port does not carry relay currents, but instead only the emitter current of a small-signal 2N3904.

Figure 7 shows the completed board. An *ExpressPCB.RRB* file is available from the author upon request.

A Final Observation

Through some alchemy of design, the Jennings vacuum relays, like the RJ1A often used in home builds, do not seem to suffer from the pathologies exhibited in **Figures 1**, **2**, and **5**.

Chuck MacCluer, W8MQW, was first licensed in 1953 as Novice Class, WN8MQW, and now holds an Amateur Extra Class license, W8MQW. He has been active in EME on 432 MHz and 1296 MHz. These days he is active with SSB, CW, and digital modes on HF, as well as rain-scatter propagation on 10 GHz. Chuck earned the PhD degree from the University of Michigan, and is now Professor Emeritus of Mathematics at Michigan State University. Chuck is a Life Member of ARRL, IEEE, and ASHRAE, and member of RSGB, SIAM.

References

[1] **https://www.w8ji.com/relay.htm**
[2] **https://www.w8ji.com/ameritron_relay_module.htm**
[3] **www.w1ghz.org/seq/Why_do_I_need_a_Sequencer.pdf**
[4] **https://www.w6pql.com/relay_sequencer.htm**
[5] **https://vhfdesign.com/other/sequencer-pcb.html**
[6] **https://eb104.ru/internet-magazin/ustroystva-dlya-zaschity-usiliteley-moschnosti/sequnser-for-all-bands**
[7] A refreshingly simple Arduino-based sequencer schematic and code is available by request from the author via email: **w8mqw@arrl.net**.

Dr. Philip Cassady, K7PEC

40106 SE 60th St., Snoqualmie, WA 98065; **pcassady@alum.mit.edu**

Combined Effects of Antenna Height and Ground Condition on the Performance of a Horizontal Dipole Antenna

Calculations reveal the effects of antenna height and ground parameters on the performance of an 80 meter horizontal dipole antenna.

It is well known that the performance of a horizontal dipole antenna depends on its height above the ground and also the electrical characteristics of the ground itself. This paper investigates the combined effects of antenna height and ground condition on the resonant frequency, the real part of impedance, the impedance phase angle, the bandwidth and the transmitted wave elevation angle for an 80 m horizontal dipole antenna cut to be resonant at 3.75 MHz in free space. The calculations were done using *4nec2*, the numerical electromagnetic code developed by Arie Voors and is available without charge at, **https://www.softpedia.com/get/Science-CAD/4nec2.shtml**.

The 80 m horizontal dipole used in these calculations had arms of #12 AWG wire each 64 ft long. The height of the dipole was varied from 25 ft (0.095 wavelengths) to 135 ft (0.51 wavelengths) above four different real ground conditions provided in *4nec2*: Perfectly Reflecting, Good (0.015 S/m conductivity, 17 dielectric constant), Moderate (0.003 S/m conductivity, 4 dielectric constant) and Poor (0.001 S/m conductivity, 5 dielectric constant).

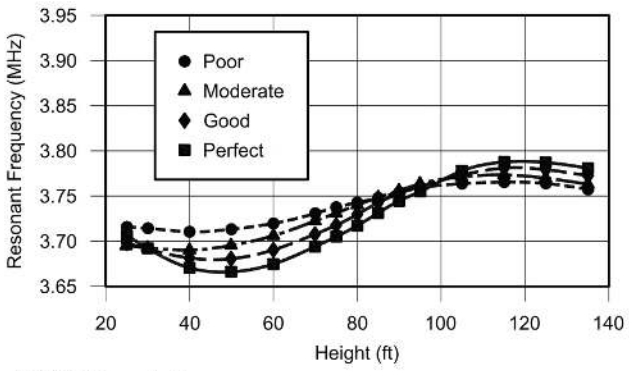

Figure 1 — Resonant frequency *vs.* antenna height.

Resonant Frequency

The combined effect of horizontal dipole antenna height and ground condition on resonant frequency is shown in **Figure 1**. Resonant frequency is the frequency where the reactive impedance passed through zero during a frequency sweep calculated by *4nec2*. The resonant frequency of this antenna in free space, without the presence of the ground is 3.745 MHz.

The current in the horizontal dipole antenna is the sum of two components: one from the transmitter and one from the RF energy reflected from the ground. The strength and phase of the reflected energy change as the antenna height is raised or the ground conditions change. The resonant frequency of the horizontal dipole increases with antenna height because the RF energy reflected from the ground changes in phase and decreases in strength at the position of the antenna. The change in phase of the reflected energy causes the initial dip in resonant frequency as the antenna height is increased, followed by the overshoot in resonant frequency at heights above approximately 95 ft (0.36 wavelengths) where the resonant frequency passes through the design frequency of 3.75 MHz. These excursions in resonant frequency decrease as the antenna height is increased and the RF

energy reflected by the ground decreases in strength. This effect of change in phase and weakening strength is greater for "Good" ground conditions than for "Poor" ground conditions because ground reflections are larger for the "Good" ground. The phase of the reflected wave at the position of the antenna is the same for all ground conditions.

Real Impedance

The combined effect of horizontal dipole antenna height and ground condition on the real part of the antenna impedance at the design frequency of 3.75 MHz is shown in **Figure 2**. The real impedance of this antenna in free space without the presence of the ground is 66 Ω.

The real impedance at 3.75 MHz increases with antenna height as the strength of the ground reflected energy decreases and its phase at the antenna position changes. The real impedance reaches a peak near an antenna height of 85 ft (0.35 wavelengths) for a perfectly reflecting ground. This effect is weaker for the "Poor" ground condition because more energy is absorbed in the poor ground and not reflected back to the antenna. Both the maximum real impedance and associated antenna height are greater as the ground condition improves from "Poor" to "Perfect."

Impedance Phase Angle

The combined effect of horizontal dipole antenna height and ground condition on the phase angle of the antenna impedance at the design frequency of 3.75 MHz is shown in **Figure 3**. The impedance phase angle of this antenna in free space, without the effect of the ground, is +1.7°.

The impedance phase angle passes through zero as the antenna passes through 3.75 MHz resonance at a height of approximately 92 ft (0.35 wavelengths) above a perfectly reflecting ground. The resonant height decreases slightly to approximately 85 ft (0.32 wavelengths) as the ground condition degrades from "Good" to "Poor."

Bandwidth

The combined effect of horizontal dipole antenna height and ground condition on the bandwidth of the dipole antenna is shown in **Figure 4**. The bandwidth is defined as the difference between the upper and lower frequencies providing an SWR of 2.0 during a *4nec2* frequency sweep. The bandwidth of this antenna in free space, without the effect of the ground, is 180 kHz.

The bandwidth does not change much with either antenna height or ground

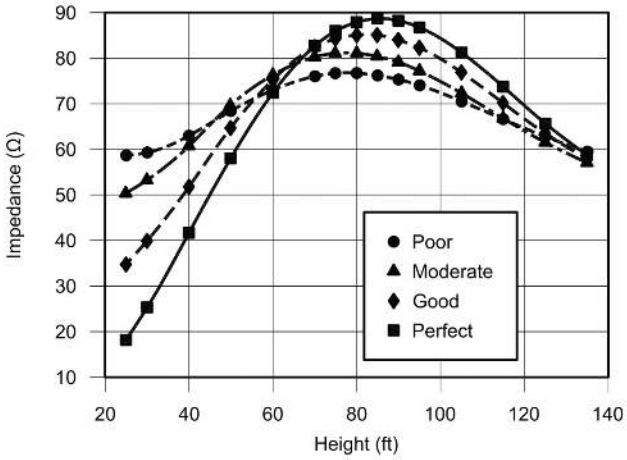

Figure 2 — Real part of impedance *vs.* antenna height.

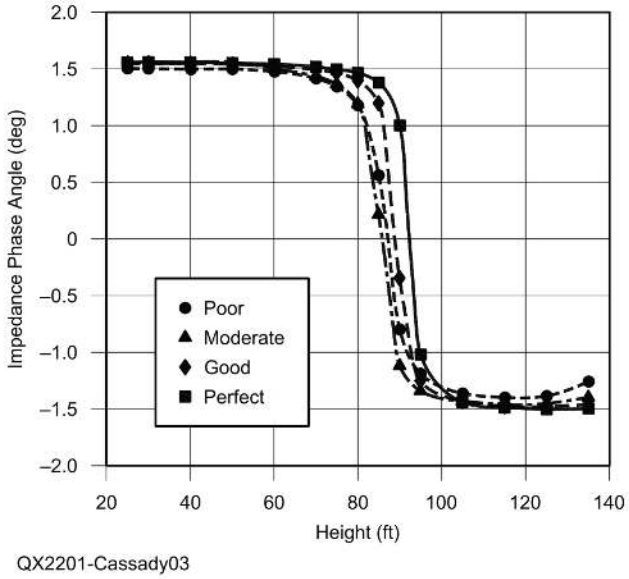

Figure 3 — Impedance phase angle *vs.* antenna height.

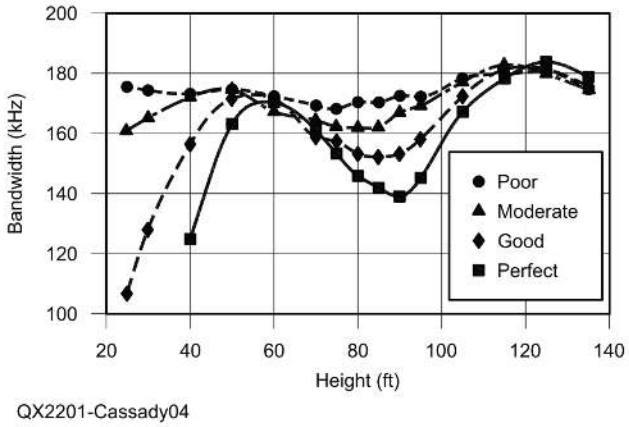

Figure 4 — Bandwidth *vs.* antenna height.

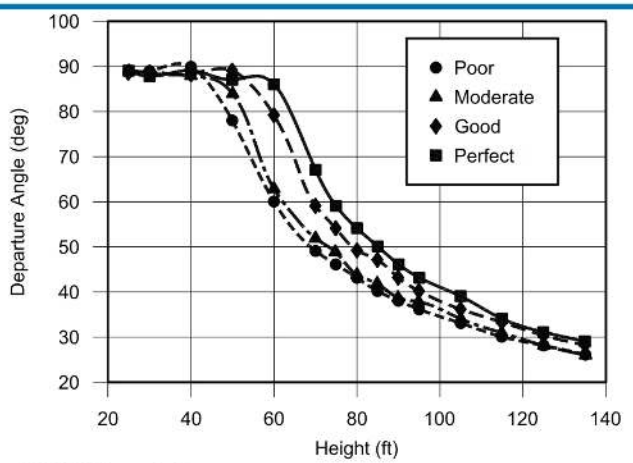

Figure 5 — Departure angle of maximum radiation *vs.* antenna height.

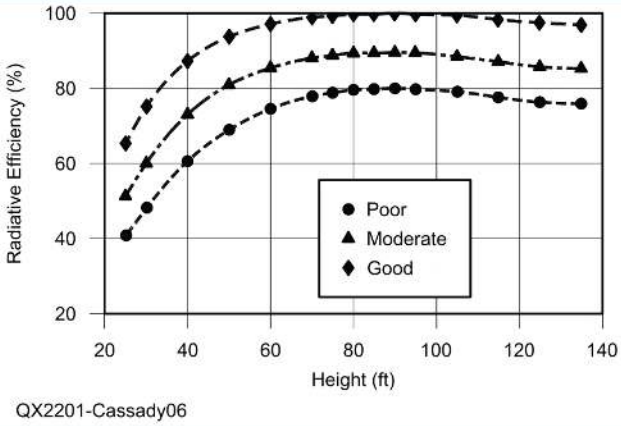

Figure 6 — Radiation efficiency *vs.* antenna height.

condition. However, at antenna heights less than about 50 ft (0.19 wavelengths) the presence of a poor ground decreases the Q of the antenna and slightly increases the bandwidth. Near the resonant height of 80 – 90 ft, this effect is repeated at reduced magnitude with the minimum bandwidth increasing and moving to lower values of antenna height as the ground condition degrades from "Perfect" to "Poor."

Departure Angle

The combined effect of horizontal dipole antenna height and ground condition on the radiation departure angle of the dipole antenna tuned to 3.75 MHz is shown in **Figure 5**. The radiation departure angle is the angle measured above horizontal calculated by *4nec2* to have the largest far field gain in the vertical plane.

The departure angle is almost straight upwards for antenna heights below 40 ft (0.15 wavelengths). This condition persists for higher antenna height as the ground condition improves from "Poor" to "Perfect." The departure angle decreases with height more quickly for "Poor" ground conditions than for "Good" conditions because the reflected wave has less power and phase coherence with the transmitted wave under these conditions. The departure angle approaches 25° to 30° regardless of the ground condition for antenna height above 135 ft (0.51 wavelengths), but the poorest ground conditions consistently provide the lowest departure angles.

Radiation Efficiency

The combined effect of horizontal dipole antenna height and ground condition on the radiation efficiency of the dipole antenna tuned to 3.75 MHz is shown in **Figure 6**. This figure shows that the amount of transmitter power lost to heating the ground increases as the antenna is lowered nearer to the ground. Regardless of the ground condition, any antenna located closer than 50 ft (0.19 wavelengths) to the ground suffers appreciable loss of transmitter power to heating the ground. The poorer ground condition increases the loss of energy to the ground and limits the radiation efficiency to 80% even at the higher antenna positions.

Conclusions

The performance of a horizontal dipole antenna located above the ground is influenced both by the radiation provided to it by the transmitter and by the its radiation reflected from the ground back up to the antenna. The permeability of the ground controls the strength of this reflected wave and the dielectric constant of the ground controls its phase.

The horizontal dipole antenna that was cut to resonate at 3.75 MHz in free space resonates at this design frequency for antenna height of approximately 95 ft (0.36 wavelengths). It resonates at a slightly lower frequency for lower heights and at a slightly higher frequency for greater heights. This effect is smaller for poorer ground conditions.

The real part of the impedance at the design frequency of 3.75 MHz rises to a peak value of 89 Ω near the antenna height of 85 ft (0.32 wavelengths) and subsequently drops for higher antenna heights. This effect is also smaller for poorer ground conditions.

The impedance angle at the design frequency of 3.75 MHz passes through zero (resonance) near the antenna height of 92 ft (0.35 wavelengths). Resonance occurs at slightly lower antenna heights for poorer ground conditions.

At heights below 50 ft (0.19 wavelengths) the bandwidth provided by this antenna decreases. Poorer ground conditions exhibit less decrease in bandwidth. A similar decrease in bandwidth occurs around the antenna height of 90 ft (0.34 wavelengths) with less decrease over poorer ground conditions.

The radiation departure angle at the design frequency of 3.75 MHz is nearly vertically upward for antenna heights below 50 ft (0.19 wavelengths). The departure angle decreases as antenna height is increased. At any antenna height the departure angle is lower for poorer ground conditions.

The radiation efficiency decreases quickly for antenna heights below 50 ft (0.19 wavelengths) and is consistently lower for all antenna heights over poorer ground conditions.

In summary, this horizontal dipole antenna passes through resonance at its design frequency of 3.75 MHz and exhibits maximum real impedance at a height near 90 ft (0.35 wavelengths) above the ground. Its bandwidth decreases and it provides a radiation angle near vertical for antenna heights below 50 ft (0.19 wavelengths) where its radiation efficiency drops abruptly.

Dr. Phil Cassady, K7PEC, is a retired Boeing Senior Technical Fellow living on a farm in rural Washington state. He is 80 years old and has been a ham for 8 years, operating only CW mostly on 40 and 80 meters. Phil holds an Amateur Extra class license, is an ARRL Volunteer Examiner, and is a member of the Straight Key Century Club. More interested in learning than operating, he has concentrated on antenna design and has constructed four horizontal and two vertical antennas on his farm property. He studied fluid dynamics, plasma physics and lasers at MIT and CalTech, and started in electronics and radio only after he retired. Phil is interested in Software Defined Radio, elk hunting and vintage motorcycles.

John Stanley, K4ERO

524 White Pine Lane, Rising Fawn, GA 30738; **jnrstanley@gmail.com**

Precautions When Using the Return Loss Method of Measuring Coax Loss

Measurements confirm that there are cases where the loss on a line with SWR is lower than on a matched line.

Steve Stearns, K6OIK, in "Loss Formulas for General Uniform Transmission Lines and Paradox 5" **[1]** presents improved formulas for calculating excess loss in transmission lines due to SWR. The article shows that there are cases where coax loss on unmatched lines can be quite different from what one would expect using the older calculation methods. The formulas implemented in the program *TLW* by Dean Straw, N6BV, also show this **[2]**. For example, one can find cases where the loss on a line with SWR is lower than on a matched line.

A commonly used method of determining "matched" loss in coax is to measure the return loss or the SWR when the coax is either shorted or open at the far end **[3]**. The new formulas show that this method must be used with caution especially for electrically short lines. Since SWR is directly related to return loss, the same precautions must be used with either SWR or return loss. I decided to check these precautions by actual measurements.

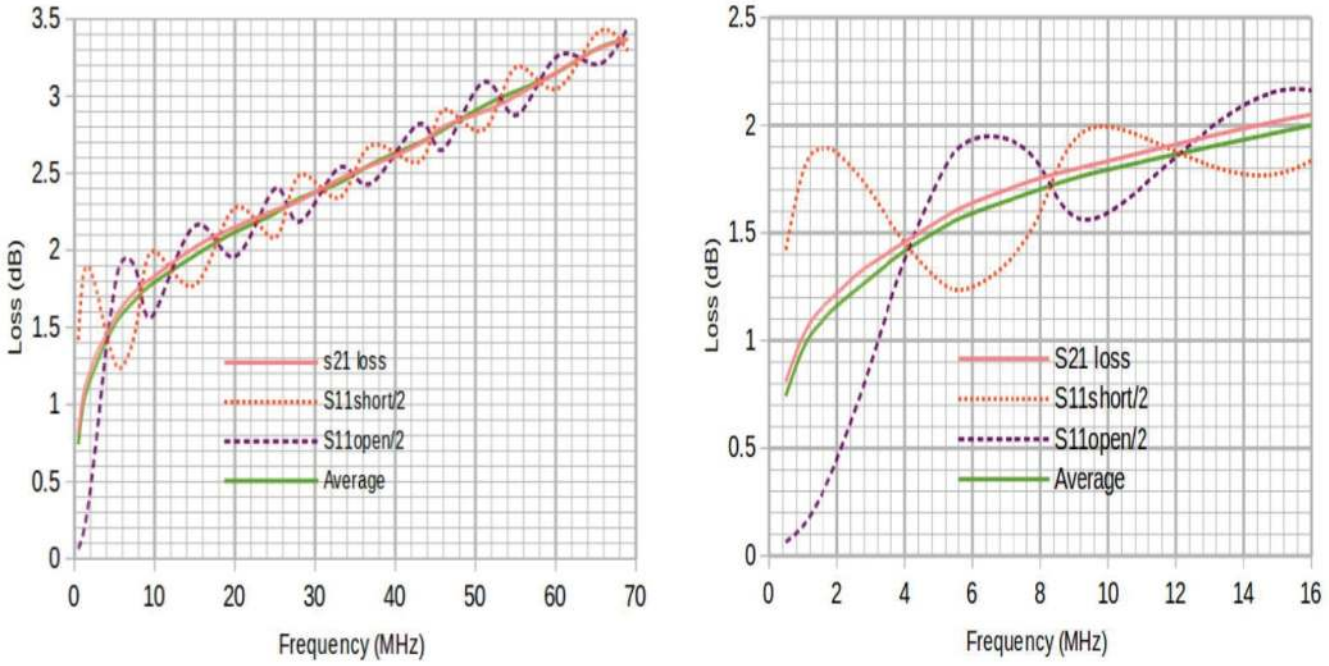

Figure 1 — (Left) Measured loss of RG-174 coax using three methods: S_{21}, half of S_{11} (short), half of S_{11} (open), along with the average of the open and short measurements; (right) expanded low frequency region.

A nanoVNA was used to measure the loss in a 20 meter (electrical) length of 1/8 inch coax similar to RG-174, using the S_{21} method, where the matched loss between two ports is measured, and also using the S_{11} or return loss method. The return loss method places either a short or an open on the far end of the coax. The coax loss is taken to be one-half of the measured return loss. Since the wave travels to the end of the line and back, the measured loss is double what it would be for a single trip. The results of the three methods are compared in **Figure 1** (graphs are from *LibreOffice Calc*).

The solid upper trace is using the S_{21} (through) method. The S_{11} short and open tests are shown by the dotted and dashed lines. Frequency is plotted from 1-70 MHz, loss from 0 to 3.5 dB. The average of these two S_{11} methods is the lower solid line.

The loss using the S_{11} method with a short on the far end measures greater loss than the S_{21} method up to 4 MHz. Between 4 and 8 MHz the measured loss is less than the S_{21} measured loss. At 4 MHz the line is about a quarter wave long. The measured value using S_{11} oscillates above and below the S_{21} value every quarter wavelength.

The S_{11} method at low frequencies using an open at the far end of the coax gives radically low loss values. Like the short method, it also gives a correct value for loss at multiples of an electrical quarter wave length of coax. However, the minimum and maximum values above and below the S_{21} values compared with the values given with the short are "out of phase." Thus when the short gives values that are too high, the open method readings that are too low, and vice versa. The good news is that if we average the short and open measured data we get a value very close to the value measured by the S_{21} method. The averaged values as shown on the graph fall on the S_{21} line to within measurement accuracy of 0.05 dB. Careful calibration of the nanoVNA, or use of a lab grade VNA, would probably have matched them almost perfectly. This validates a previously published theoretical analysis of this issue **[4]**.

The reason for this failure of the single-measurement S_{11} method, especially when using an open circuit at the far end, is that for most coaxial cables, the copper loss is far higher than the dielectric loss.

The copper loss in RG-174 is greater than the dielectric loss per unit length. This is typical of most coaxial lines. As the frequency goes higher, the dielectric losses increase faster than the copper losses, although for RG-174 it never equals it even into microwave frequencies. The inequality of the losses between the copper and the dielectric makes the measured Z_0 of the coaxial line complex. If you look at the Z_0 values for coax in *TLW*, you will see that they all have a negative jX component. This is because copper losses are larger. As you go up in frequency the line Z_0 gets closer to 50 Ω with a zero j-component. In lines with most of the loss in the copper rather than the dielectric, running the line with high voltage and low current lowers the loss. It can even lower it below the "matched loss" value in some cases.

This is reflected in the fact that the Z_0 for these cables, especially at low frequencies, is complex. Values of $50 - j12$ Ω are not unheard of. For example *TWL* gives that value for RG-174 at 500 kHz. When Z_0 of a coax has a imaginary part, it indicates that the copper loss and dielectric loss are not balanced. This is a well known issue in telephone lines.

When a short is used to test an electrically short cable, the currents in the braid and center conductor are higher than in the matched case. This leads to increased loss. This extra loss is not an artifact of the measurement method. The VNA is measuring actual loss in the cable, but this does not accurately reflect the matched loss case, where the Z value is never close to zero and thus the extreme currents will not exist. Remember that copper loss is proportional to the square of the current.

When the S_{11} method is used with a short cable with an open circuit on the end, the currents in the coax are much smaller that in the matched case. For very short cables, there will be almost no current whatsoever. Since the dielectric losses are very low, the cable loss is small. The VNA is actually measuring these very small losses, but again, this does not accurately tell us what the loss will be in a cable feeding a matched load.

If the cable is a quarter wave long the currents rise as the Z value rotates into the left hand side of the Smith Chart and the real part of Z on the line approaches zero at a quarter wave from the open. When the cable is a quarter wave multiple, we know that the shorted or open line will experience both high and low current regions equally and the S_{11} measured values will converge on the correct S_{21} measurement. The oscillations in loss persist and move depending on the line passing through the high loss region more or fewer times than it passes through the low loss region. As the line lengthens or the frequency rises, the number of trips around the Smith Chart increases. An interesting result of this phenomena is that at VHF using high power with a high SWR, by passing one's hand along a coax it is possible to feel the current nodes as warmer places on the coax. These occur every electrical half wavelength as the standing waves of current heat up the line.

The take away is that when using the return loss method of checking coax loss, one should either use a line that is a multiple of an electrical quarter wave, where the short and open will give similar values, or else take the average of the two values. This is especially important for electrically short lines. If a two-port instrument is available, using the S_{21} method is more accurate and probably easier unless it is difficult to bring both ends of the cable to the instrument.

John Stanley, K4ERO, and his wife Ruth, WB4LUA, retired to Rising Fawn, Georgia after 45 years in international broadcasting, where they did engineering, consulting, and training with Christian radio stations in many countries. As an ARRL Technical Adviser for the past 30 years, John has contributed to many ARRL publications.

Notes

[1] S. Stearns, K6OIK, "Loss Formulas for General Uniform Transmission Lines and Paradox 5," *QEX*, Sep./Oct. 2021, pp. 18-28.

[2] R. Dean Straw, N6BV, "TLW (Transmission Line for Windows): Version 3.24," Feb. 7, 2014: **www.arrl.org/files/file/QST%20Binaries/June2014/TLW3.zip**

[3] Section 23.5.4, "Testing Transmission Lines," *ARRL Antenna Book*, 22nd Ed., pp. 23-34.

[4] An analysis of the losses that shows the validity of this averaging method is explained in F. Witt, AI1H, "Measuring Cable Loss," *QEX*, May/June 2005, pp. 44-47.

Peter DeNeef, AE7PD

2302 Quail Point Circle, Medford, OR 97504; **hamradioandvision@gmail.com**

Microwave Power Density Estimation for Parabolic Dish Antennas

Three methods are used to estimate the field power density from a parabolic dish antenna.

During low power operation the microwave field near a dish antenna can exceed FCC safety limits for human exposure. I compared the results from three methods to estimate the field power density from a parabolic dish antenna:

1) Published results of a field power analysis,

2) Far field formula, the basis for the online ARRL RF calculator, and

3) FCC formula for aperture antennas.

Published Analysis

I used power density estimates from an analysis by George Kizer **[1]**, **[2]**, **[3]**. He uses analytic methods to calculate the diffraction fields for the aperture of a circular parabolic dish. The analysis includes formulas for power density in terms of the gain, dish diameter, frequency, power, and distance from the antenna.

The power density in front of dish antennas is highest along the beam axis perpendicular to the center of the dish. **Figure 1** shows the estimated power density S (mW/cm^2) *vs.* distance d, ft, from the center of a 2 ft diameter 10 GHz dish when the average input power to the antenna is 1 W, the power loss in the antenna is negligible, and the aperture efficiency (discussed below) is 0.55.

The near-field power density on the axis is essentially constant at 2.5 mW/cm^2. The near field region is followed by a transition where the power density decreases with distance from the antenna. In the far field region, S is proportional to d^{-2} as the beam broadens. The log-log graph of S *vs.* d is a straight line.

The FCC exposure limits for frequencies from 1.5 GHz to 100 GHz are 1 mW/cm^2 for General Population exposure and 5 mW/cm^2 for Controlled exposure that applies to amateurs and family members **[4]**. The averaging times are 6 minutes for Controlled exposure and 30 minutes for General Population exposure. For 1 W average power the maximum near field power density of 2.5 mW/cm^2 in **Figure 1** exceeds the FCC limit for General Population exposure, and it complies with the limit for Controlled exposure.

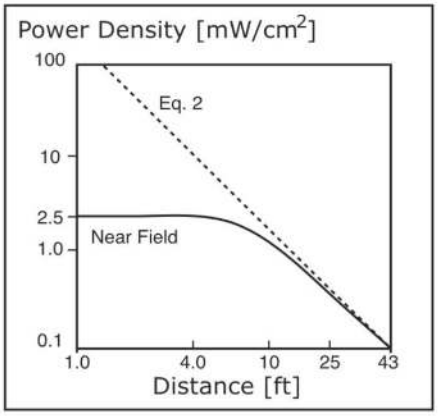

Figure 1 — Power density S (mW/cm^2) *vs.* distance d (ft) from a 2 ft diameter dish antenna is shown for P = 1 W and η = 0.55; based on data from [1], [2], [3].

Aperture Illumination Efficiency

Aperture illumination efficiency is a key factor that determines near-field power density and far-field gain. The physical aperture of a parabolic dish is the planar area defined by the edge of the dish. Aperture illumination is the pattern of radiation at the aperture after it has been reflected by the dish. For an ideal antenna with maximum gain the intensity and phase of the illumination are uniform at the aperture. To reduce side lobes in the far field pattern the designers of commercial antennas sacrifice some gain by tapering the spatial distribution of illumination from a maximum in the center to a lower level at the edge.

For an antenna that is nearly lossless the aperture illumination efficiency η is the same as the antenna efficiency. It is defined as the gain divided by the maximum gain with a uniformly illuminated aperture. When the aperture is uniformly illuminated, $\eta = 1.0$. In general, the gain is **[2]**, **[4]**, **[5]**,

$$G = \frac{4\pi\eta A}{\lambda^2} \qquad (1)$$

where A is the area of the aperture and λ is the wavelength. You can use **Eq. (1)** to estimate η. For example, η = 0.55 for a 2 ft diameter, 10 GHz dish with 10 log(G) = 33.5 dBi.

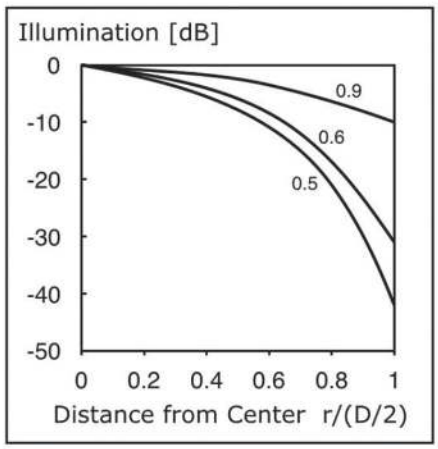

Figure 2 — Aperture illumination (dB relative to the center) *vs.* radial distance from the center of the aperture (normalized to the edge at radius *D*/2) is shown for aperture illumination efficiencies $\eta = 0.5$, 0.6, and 0.9; data from [2].

Table 1 — Maximum antenna input power not exceeding the FCC MPE (maximum permissible exposure) limits. Dish diameter is *D* (ft), and aperture illumination efficiency $\eta = 0.55$; data from [1], [2], [3].

D, ft	*General Population Limit, W*	*Controlled Limit, W*
1	0.1	0.5
2	0.4	2.0
3	0.9	4.5
4	1.6	7.9
6	3.6	18
8	6.3	32
10	9.8	49

Figure 2 shows examples of aperture illumination profiles and efficiencies used in the analysis. Illumination in dB relative to the center of the aperture is shown *vs.* distance from the center, normalized to the aperture radius *D*/2. The profiles shown for $\eta = 0.5$ and 0.6 are similar to the actual illumination in typical commercial antennas.

Compared with uniform illumination, power density on the axis is higher when the illumination is tapered (lower η) **[1]**, **[2]**, **[3]**.

Maximum Permitted Input Power

Table 1 shows estimates of the maximum input power that does not exceed FCC power density exposure limits in the near field of an essentially lossless antenna with $\eta = 0.55$ **[1]**, **[2]**, **[3]**. The limits depend on the dish diameter *D*, ft, and they are independent of frequency. Aso see the Sidebar – **Sometimes SAR Applies.**

The table shows power limits for General Population and Controlled exposure. The permitted power increases for larger dishes, as the power is distributed over a bigger area.

Far Field Power Density Estimates

The ARRL RF exposure calculator is based on a far-field model for power density **[6]**, **[7]**, **[8]**. When ground reflections can be neglected the estimated far field power density *S* is given by,

$$S = \frac{PG}{4\pi d^2} \qquad (2)$$

where *P* is average power. The ARRL Lab has shown that this model can provide useful, conservative *near* field exposure estimates for a variety of amateur radio antennas.

The dashed line representing **Eq. (2)** in **Figure 1** shows that the far-field model and Kizer's analysis agree in the far field. **Eq. (2)** is increasingly conservative (higher power density than estimated by analysis) as you move closer to the antenna.

For the purpose of estimating power density the FCC formula for the distance to the far field boundary is **[4]**,

$$R_{ff} = \frac{0.6D^2}{\lambda} \ . \qquad (3)$$

Eq. (3) gives $R_{ff} = 24$ ft for a $D = 2$ ft diameter, 10 GHz antenna. As shown in **Figure 1**, this is consistent with the results of Kizer's analysis. **Figure 3** shows R_{ff}, ft *vs.* frequency *f*, GHz, for parabolic dish antennas with diameters $D = 2$ ft, 4 ft, and 6 ft.

FCC Near Field Estimate

An FCC formula to estimate the near field power density for an aperture antenna is **[4]**,

$$S_{nf} = \frac{16\eta P}{\pi D^2} \qquad (4)$$

where the aperture efficiency is typically 0.5 to 0.75. **Eq. (4)** gives $S_{nf} = 0.75$ mW/cm^2 for a 2 ft dish with $\eta = 0.55$ and $P = 1$ W. This is lower than the level shown in **Figure 1**, where the maximum near field power density is 2.5 mW/cm^2. Also, **Eq. (4)** fails to account for the increase in S_{nf} when aperture efficiency is decreased.

Home-Built Dish Antennas

The power limits in **Table 1** apply to commercial antennas with almost no power loss and a tapered aperture illumination profile with $\eta = 0.55$. For a typical home-built antenna the illumination profile is somewhat more uniform. Paul Wade, W1GHZ, explains in **[5]** that a rule of thumb for amateur antennas is to use an illumination profile that is down 10 dB at the edge. For the profiles shown in **Figure 2** this corresponds to an illumination efficiency of 0.9.

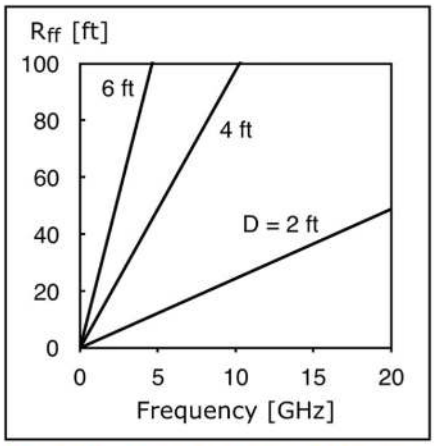

Figure 3 — Estimated distance to the far field boundary R_{ff} (ft) *vs.* frequency (GHz) is shown for three parabolic dish diameters *D* (ft), calculated using Eq. (3).

Also, power loss can be significant if there is "spillover" of feed horn radiation directed outside the edge of the dish. For an electrically lossy antenna the radiated power $P_{rad} = kP$, where *P* is the power to the antenna and *k* is the efficiency due to power loss. In that case, in **Eq. (1)** the illumination efficiency η is replaced with the total antenna efficiency $\eta_T = k\eta$. W1GHZ reports that for amateur antennas $\eta_T = 0.55$ is reasonable **[5]**. He adds that some references state that η_T between 0.7 and 0.8 can be achieved with a very good feed system.

I calculated input power limits for lossy antennas with more uniform aperture illumination than Kizer's examples in **Table 1**. **Table 2** shows the maximum input power not exceeding FCC power density limits, assuming $\eta = 0.9$ and $k = 0.9$ ($\eta_T = k\eta = 0.8$). Details of my calculations are in the **Appendix**.

The limits on input power in **Table 2** are higher than in **Table 1**. This example demonstrates the convenience and usefulness of **Table 1** for estimating conservative (low) limits on the input power to antennas that have more uniform aperture illumination ($\eta > 0.55$).

Conclusions

These examples show that during low power operation the near field power density

Table 2 — Maximum antenna input power not exceeding the FCC MPE (maximum permissible exposure) limits. Dish diameter is *D* (ft); aperture illumination efficiency η = 0.9; and power loss efficiency *k* = 0.9.

D, ft	*General Population Limit, W*	*Controlled Limit, W*
1	0.2	0.9
2	0.7	3.6
3	1.6	8.2
4	2.9	15
6	6.6	33
8	12	58
10	18	91

Sometimes SAR Applies

Per FCC regulations for very close exposures, at distances less than 20 cm (0.66 ft), SAR (specific absorption rate) must be used as an exposure determiner instead of MPE (maximum permitted exposure). Distance, in this case, is the shortest distance between the radiating structure and any part of a human body.— *Ed.*

of a parabolic dish antenna can exceed FCC limits. Comparisons with different size dishes show that the maximum power permitted by FCC exposure limits is lower for smaller dishes, and it is independent of frequency.

Near field power density depends on the aperture illumination efficiency. For typical commercially designed dish antennas with almost no power loss the analysis by Kizer for dishes with η = 0.55 provides estimates of the maximum antenna input power permitted by FCC exposure limits (**Table 1**). These estimates are conservative (low) limits for antennas with more uniform aperture illumination (η > 0.55).

The far field model used in the ARRL RF exposure calculator provides accurate estimates for power densities and separation distances in the far field of a parabolic dish.

Appendix – Estimating Power Density for Parabolic Dish Antennas

This appendix shows how to calculate the power limits in **Table 2**. For different dish diameters the table lists maximum input powers not exceeding FCC power density limits. The formulas are from **[2]**. The examples in the table are for a circular parabolic dish antenna with aperture illumination efficiency η = 0.9 and power loss efficiency $k = 0.9$.

The FCC power density limit for microwaves is 1 mW/cm² for General Population exposure and 5 mW/cm² for Controlled exposure **[4]**. Eq. (8.76) in **[2]** gives the maximum near field power not exceeding the FCC limit for General Population exposure:

$$P_{dBm} = 36.75 + 20\log(D_{ft}) - 10\log(\eta) - P_{NNFL} \quad (5)$$

where P_{NNFL} is the normalized near field power density in dB from Eq. (A.93) in the Appendix of **[2]**:

$$P_{NNFL} = A + B\eta + \frac{C}{\eta} + D\eta^2 + \frac{E}{\eta^2} + F\eta^3 \quad (6)$$

where:
$A = +40.430453$
$B = -61.480406$
$C = -0.46691971$
$D = +55.376708$
$E = +0.04791274$
$F = -19.805638$.

Table 2 is for antennas that are electrically lossy ($k = 0.9$). The input power to the antenna P_{IN}, W, and the power radiated P_{RAD}, W, are related by $P_{RAD} = kP_{IN}$. P (in dBm) in **Eq. (5)** is P_{RAD}. To calculate P_{IN}, W, for the table, convert P(in dBm) from **Eq. (5)** to watts and divide the result by 0.9.

The preceding equations are for General Public Exposure. For Controlled exposure the FCC limit on power density is 5 times the limit for General Public exposure. Power density is linearly proportional to the transmitted power, so the limit P, W, for Controlled exposure is 5 times P, W, for General Public exposure from **Eq. (5)**. This is equivalent to adding 7 dB to P (in dBm) in **Eq. (5)**.

To test **Eq. (5)**, I recalculated one of the limits in **Table 1** for η = 0.55 and $k = 1.0$ from **[1]**, **[2]**, **[3]**. For η = 0.55, **Eq. (6)** gives $P_{NNFL} = 19.38$ dB. For $D = 2$ ft, **Eq. (5)** is,

$$P_{dBm} = 36.75 + 20\log(2) - 10\log(0.55) - 19.38$$
$$= 26.0 \text{ dBm}$$
$$P_W = 0.4 \text{ W}.$$

This agrees with the General Public Exposure limit in **Table 1** for $D = 2$ ft.

Peter DeNeef, AE7PD, received his first license as KF7FPX in 2009. He has written about RF exposure safety for QEX *(Nov/Dec, 2017 and Mar/Apr, 2021), as well as articles about international RF safety guidelines of the International Commission on Non-Ionizing Radiation Protection (ICNIRP). More of his articles can be found on his popular web site for vision-impaired hams,* ***www.HamRadioAndVision.com****.*

References

[1] G. Kizer, "Microwave Antenna Near Field Power Estimation," *Proceedings of the 4th European Conference on Antennas and Propagation*, 12-16 Apr. 2010. pp. 1-5. **https://ieeexplore.ieee.org/document/5505204**.

[2] G. Kizer, "Digital Microwave Communication: Engineering Point-to-Point Microwave Systems," Wiley-IEEE Press, 2013, pp. 249-319.

[3] G. Kizer, "Antenna Near Field Power Density Public Safety Limits," *NSMA Annual Conference*, May 17-18, 2016; **www.nsma.org/wp-content/uploads/2016/06/NSMA-RF-Public-Safety-Antenna-Near-Field_George-Kizer.pdf**

[4] "Evaluating Compliance with FCC Guidelines for Human Exposure to RadioFrequency Electromagnetic Fields," *OET Bulletin 65 (1997); currently under review*; **www.fcc.gov/bureaus/oet/info/documents/bulletins/oet65/oet65.pdf**.

[5] P. Wade, W1GHZ, "The W1GHZ Online Microwave Antenna Book, 2006," **www.w1ghz.org/antbook/contents.htm.**

[6] E. Hare, W1RFI, "Understanding the Changes to the FCC RF Exposure Rules," *QST*, Sep. 2021 pp. 60-62.

[7] E. Hare, W1RFI, *RF Exposure and You, ARRL, 1998*, reprinted 2003, currently under review. **www.arrl.org/files/file/Technology/RFsafetyCommittee/RF+Exposure+and+You.pdf**

[8] **www.arrl.org/rf-exposure-calculator**.

Alan Victor, W4AMV

8809 Ross Ct., Raleigh, NC 27613; **avictor73@hotmail.com**

Unraveling the Links in Link Coupled Circuits

An investigation of the transformer coupled tuned impedance transforming circuit.

The magnetically coupled inductors that form a transformer impedance modification circuit are investigated. Several forms of the circuit containing two inductors which are linked by their mutual inductance exist. **Figure 1** illustrates a variety of forms which include the tuned primary/tuned secondary, the tuned primary untuned secondary and their variations where the tuning is accomplished by either parallel or series resonant circuit arrangement. Circuit parameters include the primary and secondary inductance, *L*1 and *L*2. Their coupling factor *k* or mutual inductance and the resonating capacitance. The circuit problem is finding these required parameters at a given frequency that provide transferring *RL* to a specified ZIN.

There is significant prior work on the subject of tuned coupled networks **[1]**, however recent interest surfaced in **[2]** whereby a technique applied to wideband microwave MMICs was presented. Circuit applications include push-pull as well as single-ended impedance matching. Applications are seen in oscillators, power amplifiers, tuned amplifier cascades, antenna matching and anywhere a high-to-low impedance transfer is required. Maresca in **[3]** presented a variety of designs and the solutions to the circuit parameters for a given source resistance, *Rs* and load impedance, *RL*, at a given frequency. **Figure 1B** was addressed in significant detail in **[2]**.

In this paper focus is on the third configuration, **Figure 1C**. The main interest and focus in this paper is in providing a variable impedance transfer for a specified range of high ZIN for a fixed value of *RL*. The circuit will not be constrained by the physical construction of the linked coils. For example, no variable link is required and the recalculation for a new set of coupled inductors with proper spacing is not needed. The application provides a sort of load pull or variable impedance for a pair of push-pull devices. The circuit requirement in my case is a push-pull vacuum tube, type 832A, that is operating at 7 MHz and is part of a homebrew VFO exciter.

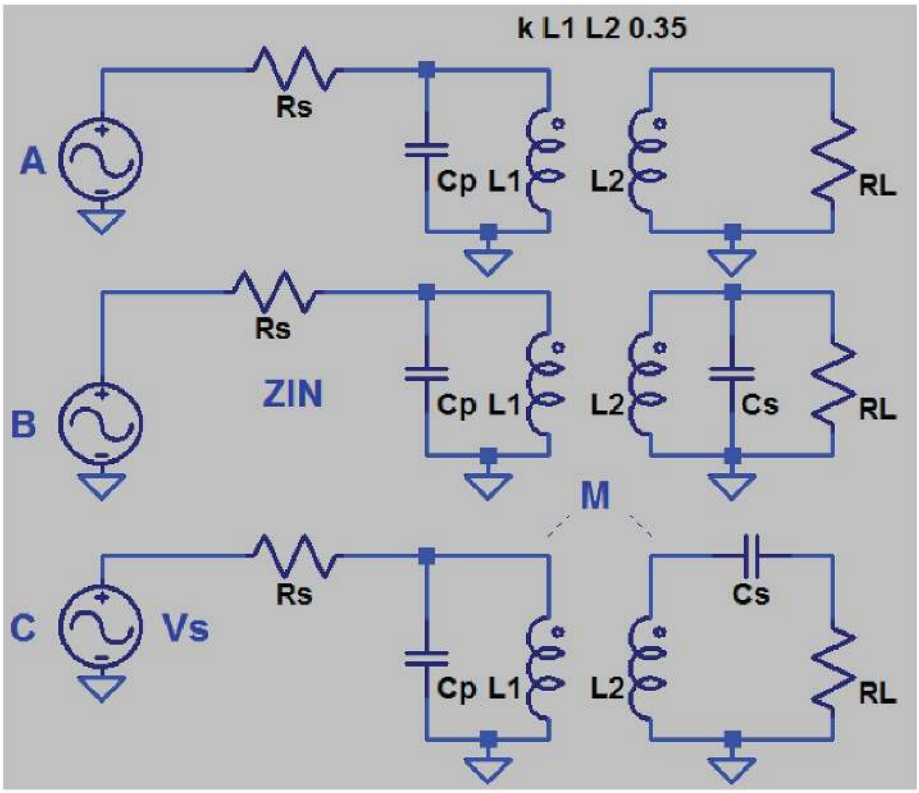

Figure 1 — Various forms of transformer link coupled circuits.

The process started by completion of calculations for the tube plate to plate impedance and finding the required component values based on **Figure 1A**, the first circuit. This circuit provided starting seed values for the coil construction. After completion of the amplifier, the power output was lower than expected, so a means of reevaluating the plate to plate load impedance is desired. Investigation of the data sheet indicates that depending on the application and the type of service, the plate to plate load impedance could vary from 3.7 kΩ to 9.5 kΩ. There was no desire to reconstruct the link coupled network or trying to produce a variable link. I desired a simpler solution and ideally one that used the current network and keeping it intact.

Varying the *Z* transfer in a simple manner

Although I started with the first circuit of **Figure 1A**, it occurred that possibly transforming the load *RL* to a new value could possibly be used to alter ZIN while maintaining all of the parameters of the network already constructed. The antenna impedance, *RL*, in the usual case is 50Ω. It needed to be transformed up in value to ZIN with nearly a 4:1 range in *Z*, but how? The third circuit of **Figure 1C** had the idea in place with the addition of a series *Cs*. However, the calculations needed to proceed without altering all the values of my current network. I needed to investigate holding the transformer coupled coil parameters constant and only permitting alterations in the *Cp* and *Cs* values to meet a range of ZIN for a specified *RL* value. The circuit analysis of such an arrangement is fairly straightforward and leads to some interesting outcomes.

Analysis of the coupled transformer

The coupled transformer circuit is shown in **Figure 2**. The load *RL* is now replaced with a series complex load of *R*L and a series reactance *X*s. The input *Z* desired is ZIN. The real part of the load can be 50 Ω, the antenna, while the series reactance might be tuned to achieve a desired ZIN. This reactance is not signed and may be inductive or capacitive. The mutual inductance, *M*, is set by the proximity of the inductors to each other and their coupling factor *k* and the individual inductances, *L*1 and *L*2. The primary and secondary currents are taken in an arbitrary manner. The linkage caused by the current in the first loop, *I*1, is directed to influence the current in the second loop, *I*2, via the mutual inductance *M*. Writing the two loop equations gives the following for loops 1 and 2.

$$V_s = I1\left(j\omega L1\right) + I2\left(j\omega M\right) \tag{1}$$

$$0 = I1\left(j\omega M\right) + I2\left(j\omega L2 + X_s + RL\right) \tag{2}$$

where $M^2=k^2L1L2$, and *X*s may be $j\omega L$ or $1/j\omega C$ and $\omega=2\pi \times$ frequency (Hz), the angular frequency. Solving for *I*2 in the second equation and substitution into the first gives,

$$V_s = \left(j\omega L1\right)I1 + \frac{\left(\omega M\right)^2}{\left(j\omega L2 + X_s + RL\right)}I1 \tag{3}$$

$$\frac{V_s}{I1} = \text{ZIN} = \left(j\omega L1\right) + \frac{\left(\omega M\right)^2}{\left(j\omega L2 + X_s + RL\right)} \tag{4}$$

Notice that *X*s can take any sign and is either additive or subtractive from $j\omega L2$. That is to say *X*s = $j\omega L$s or *X*s = $-j/\omega C$s. Hence ZIN is

$$\text{ZIN} = \left(j\omega L1\right) + \frac{\left(\omega M\right)^2}{j\left(\omega L2 + X_s\right) + RL} \tag{5}$$

where *X*s = ω*L*s or $-1/\omega C$s. ZIN has two components. The self-impedance from *L*1 and the reflected impedance from the output load to the input. This reflected impedance is in series with the primary coil inductance, *L*1. The real and imaginary components of ZIN are found by multiplying just the reflected impedance by its complex conjugate,

$$\text{ZIN} = \left(j\omega L1\right) + \frac{\left(\omega M\right)^2}{j\left(\omega L2 + X_s\right) + RL}\left(\frac{RL - j\left(\omega L2 + X_s\right)}{RL - j\left(\omega L2 + X_s\right)}\right) \tag{6}$$

The real part is isolated,

$$\text{Re}\{\text{ZIN}\} = \frac{\left(\omega M\right)^2 RL}{\left[\left(\omega L2 + X_s\right)^2 + RL^2\right]} \tag{7}$$

and its imaginary part is added to $j\omega L1$,

$$\text{Im}\{\text{ZIN}\} = j\omega L1 + \left(-\omega^2 M^2\right)\left(\frac{\omega L2 + X_s}{\left[\omega L2 + X_s\right]^2 + RL^2}\right) \tag{8}$$

The value of *RL* is always positive and the value of Re{ZIN}will always have $\text{Re}\{\text{ZIN}\} \geq 0$. However in **(8)**, the sign of *Xs* can be positive or negative. Hence a capacitive load will reflect an inductive series component added to *L*1. Otherwise, an inductive load will reflect a series capacitive component with *L*1 and a reduction in the series primary reactance. If *Xs* is set equal to ω*L*2 at some frequency and their sum is zero, then the reflected component of Re{ZIN} reduces to

$$\text{Re}\{\text{ZIN}\} = \frac{\left(\omega M\right)^2}{RL}. \tag{9}$$

The imaginary portion of ZIN is just $j\omega L1$. Notice that in **(9)** Re{ZIN} is inversely proportional to *RL*. Because there is now a variable series resistance reflected to the input side of the transformer, the input Q is modified. However, if (ω*L*2+*Xs*) is greater than *RL*, then the reflected resistance is directly proportional to *RL*. Again, the input Q is modified. If the value of the *Xs* component tends to zero, then the resulting input impedance will tend to the results provided by the circuit of **Figure 1A** as presented in **[3]**. Key to realizing the modification of the input impedance and the ability to create a varying load impedance, is the ability to modify the series input Q of the circuits of **Figure 1**.

A special case to check and verify is the validity of the ZIN in **(6)** and consider the ideal transformer. This case sets the primary and secondary coil linkage to 100% and $k = 1$. Hence M^2 is *L*1*L*2. For simplification, assign (*Xs* + *RL*) to a load termination, *Zt*. Then the ZIN equation is

$$\text{ZIN} = j\omega L1 + \frac{\left(\omega M\right)^2}{\left[j\left(\omega L2 + Zt\right)\right]}. \tag{10}$$

This simplifies to

$$\text{ZIN} = \frac{L1}{L2}\frac{Zt}{\left[1 + \frac{Zt}{j\omega L2}\right]}. \tag{11}$$

If $j\omega L2$ is large, for example both inductors are wound on high permeability material then,

$$\mathrm{ZIN} = \frac{L1}{L2} Zt \qquad (12)$$

and since the value of the inductance, L is proportional to the turns squared, **(12)** is given by $\mathrm{ZIN} = n^2 Zt$, with $L1 > L2$, or an impedance step up.

Obtaining a variable input impedance

The ability to vary the load impedance either to a vacuum tube or a solid state device in a power amplifier is key to seeking the desired output power and improved efficiency. The link coupled transformer as an impedance transfer network is a topology that lends itself to push-pull application. Furthermore, it provides a balance to unbalanced or balun function. Investigation of the varying input Z is best undertaken by building a simple spreadsheet, available at **www.arrl.org/QEXfiles**, to handle the completed ZIN equation.

The reflected impedance is always added to the self-impedance, $j\omega L1$. So the majority of the calculation entails just the reflected impedance. The reflected ZIN is in series with $L1$ and it contains a series real R and X. Once the values of series R and X are obtained, the total X series is calculated, then conversion to the input parallel equivalent Z is required. This is obtained in the conventional manner of converting from series to parallel form by application of the (Q_s^2+1) formulation **[4]**. The case studied for my application obtained the series X on the secondary side as an air variable capacitor. As previously mentioned, if the series X on the secondary side is a capacitor, then the reflected reactance is inductive. See **Figure 3** and the final reflected form, **Figure 4**.

The value of Qin, the series Q to the right of Cp, is dependent on the value of the reflected R. Hence the resonant frequency will be shifted slightly from the usual LC product due to losses. The $L_{\mathrm{reflected}}$ value is added to $L1$ and the Qin value found from the ratio of the total (*inductive reactance*)/ $R_{\mathrm{reflected}}$. The corrected resonant frequency for **Figure 4** is of the form,

$$\omega_0 = \frac{1}{\sqrt{LC}}\left(1 - \frac{C}{L}R^2\right)$$

where the desired C, Cp is found from,

$$C_p = \frac{1}{\left[\omega_0^2\left(L1 + L_{\mathrm{reflected}}\right) + \dfrac{R^2_{\mathrm{reflected}}}{L1 + L_{\mathrm{reflected}}}\right]}. \qquad (13)$$

These calculations are all conveniently handled in spreadsheet form, **Figure 5** and **6**. The initial LC values for the linked coupled network are obtained using the first circuit **Figure 1A**, and then the method provided in **[3]**. Next, the link coupled network is constructed and measured. Its parameters are entered into the spreadsheet. Then Cs is added and incremented over a range of values and the observed values for Rp, the actual device real load resistance or ZIN, is displayed. A further check on the validity

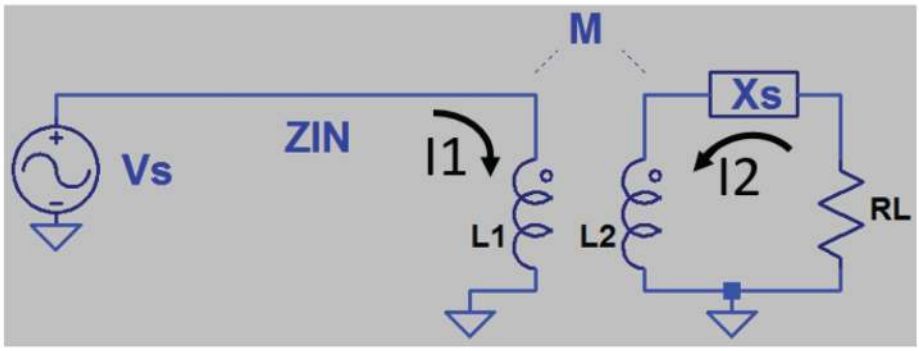

Figure 2 — Mesh circuit setup for finding ZIN.

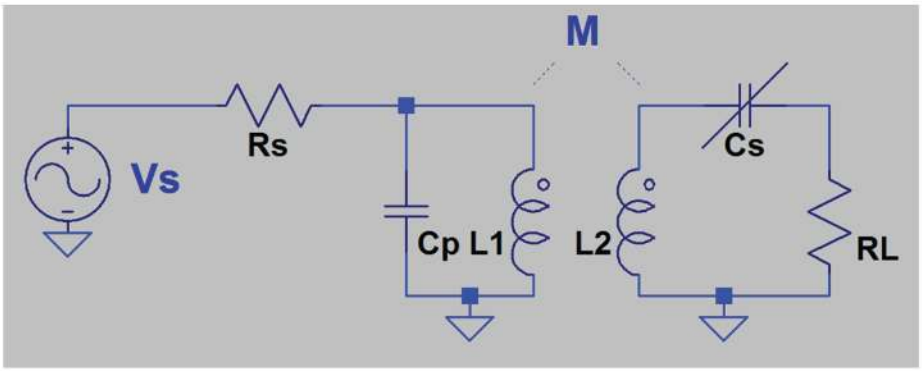

Figure 3 — Parallel resonant primary, series resonant secondary link coupled.

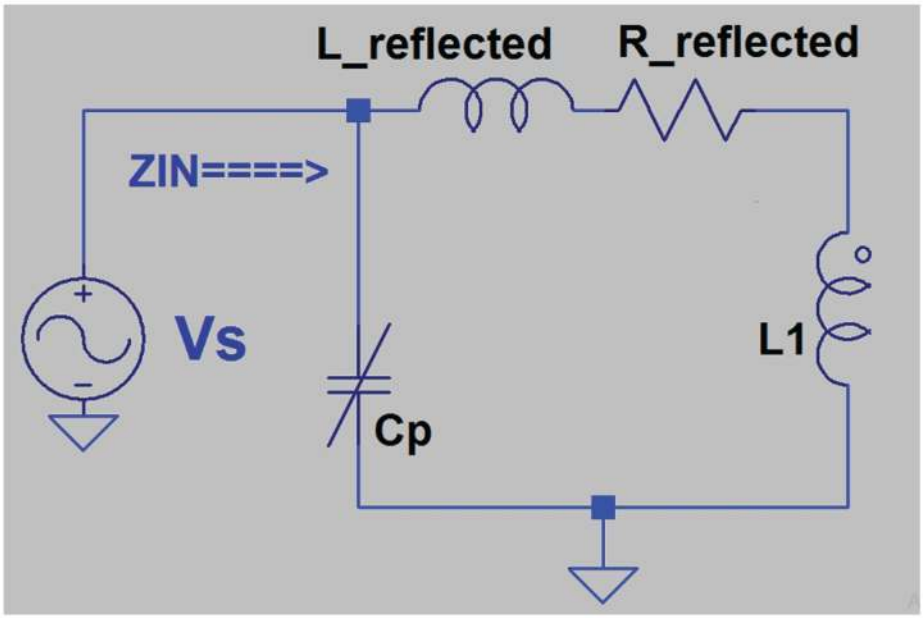

Figure 4 — Reflection of the secondary circuit to the primary.

is obtained from a linear simulation and the S-parameters are called upon to demonstrate the accuracy via the return loss provided.

While **Figure 1C** could be used directly, the results using **[3]** are only close estimates if Q values are small. I found using the first circuit of **Figure 1A** more straightforward, providing excellent agreement with simulation and measured results. Then to get the desired range of impedances, modify circuit **Figure 1A** to that of **Figure 1C** and sweep the desired series *C* values to produce an array of ZIN values or plate load impedances. These will be both above and below the desired targeted plate *Z* value. The entries to the spreadsheet for sweeping series *C* are the measured *L*1, *L*2, their coupling factor *k*, and the operating frequency. An example follows.

Example calculations and simulation

A push-pull 832A tube is operated at a plate voltage *Eb* of 500 V and an estimated plate current *Ib* of 100 mA. The plate to plate load *Z* is calculated from 2×(570 × *Eb/Ib* or 5.7 kΩ. The correction factor, 570, takes into account the relation between peak fundamental plate current, and a typical class C conduction angle of about 140°, and the dc plate current.

A spreadsheet based on **[3]** for the parallel resonant primary and untuned secondary, **Figure 1A**, is used to obtain the link coupled transformer parameters, **Figure 5**. The key resulting elements are 13.86 µH primary *L*1 and 0.91 µH secondary *L*2 with a coupling *k* factor of 0.35. The coupling factor is reasonable and an estimate based on prior work and a typical value seen with stock linked coupled inductors. The *Cp* resonating primary capacitor is 40 pF.

The link coupled coil primary and secondary are constructed based on the solenoid equation and the link coil is turned atop the primary and centered. However, several parameters have now changed. First, the circuit required a reevaluation of the plate *Z*. Second, the actual link coupled coil constructed had measured parameters, which missed the target and would require a reconstruction.

First, the plate supply voltage could not support the plate current and the plate voltage sagged due to other stages taking their share of power. A better target for the plate *Z* is revised to assist and *Eb* is reduced to a range

	A	B	C	D	E	F	G	H	I	J
1	Case I Link Coupled Tuned Primary Untuned Secondary									
2	Q1	10							Freq	7.00E+06
3	Q2	0.8								
4	R1	5.70E+03								
5	R2	50								
6	Xc1	5.70E+02								
7	XL1	609.505								
8	XL2	40								
9	k	0.353553	Keep k < 0.4 and increase Q1 if needed							
10										
11	C1	39.91	pF							
12	L1	13.86	uH							
13	L2	0.91	uH							
14										

Figure 5 — Spreadsheet setup for solving iterative cases for component parameters.

	A	B	C	D	E	F	G	H	I	J	K	L	M	N	O
2	Freq	7.00E+06	40 meters		L1	9.30E-06	XL1	4.09E+02							
3					L2	1.40E-06	XL2	6.15E+01							
4					k	0.436									
5					RL	50									
6					omega F	4.40E+07									
7		CASE I LINK COUPLED TUNED PRIMARY UNTUNED SECONDARY... Calculations from Measured Data													
8			(Ctrl)		Q2	1.23E+00									
9					Q1	9.52E+00									
10															
11					Rp	3.93E+03	This is not an exact or correct result!								
12					M_sq	2.48E-12									
13					Z_f_RE	3.80E+01	This is the series RE part of the load RL reflected to the input								
14					Z_f_IM	-4.68E+01									
15					Z_f_IM	3.62E+02	This is the FINAL series IM part of the input					Effective L	8.24E-06		
16					Qin	9.52E+00						Effective L2 inductance is above			
17					Rp	3.48E+03	This is the correted result!								
18					C_res	6.22E-11	Next need to find the corrected resonanting capacitor for primary								
19															
20	Enter the C series secondary C here				Input here a series secondary coupling capacitor and recalculate the Rp and C_res Cap										
21		C2 in pF here---------	3.30E+02		C2_pF	3.30E-10	this is the added C coupling								
22					X2	-6.89E+01	this is its reactance								
23					Z_f_RE	9.36E+01	this is the reflected series real part								
24					Z_f_IM	1.38E+01									
25					Z_f_IM	4.23E+02	this is the new final series primary L reactance					Effective L1		9.61E-06	
26					Qin	4.51E+00									
27		Here is the key outputs Rp------			Rp	2.00E+03									
28		Here is the key outputs Cres----			C_res	5.13E-11									

Figure 6 — Spreadsheet finds the array of ZIN values for successive *Cs* values. The input fields are measured transformer link coupled parameters, *L*1, *L*2 and *k*.

of 360 to 475 V at 75 mA. The plate *Z* is now in a range of 5.4 kΩ to 7.2 kΩ. Second, the measured link coupled parameters are $L1 = 9.3$ µH, $L2 = 1.4$ µH and a $k = 0.436$. There was a desire to not reconstruct the link coupled system, but to adapt to the design needs. To this end, investigation of adding a series capacitor to the link occurred. The spreadsheet is developed and based on the prior discussions proved to be invaluable at arriving at a solution.

Input frequency, 7 MHz, is in the 40-meter band and the measured link coupled parameter are used as obtained from the construction. Namely, $L1 = 9.3$ µH, $L2 = 1.4$ µH and a $k = 0.436$. The termination *RL* is 50 Ω. The plate *Z* provided by such a system would be 3.5 kΩ. Raising this ZIN to the desired level is key, and a quick sweep of values is easy to obtain. The addition of a series 180 pF readily permits a ZIN of 5.8 kΩ, **Figure 6**.

The input Q, Qin is acceptable at 12.8 and the resonating *Cp* is 50 pF. Obtaining a sweep of plate impedance values or ZIN *vs.* *Cs* is easy. As well, the Qin and resonating capacitor *Cp* are provided, see **Figures 7**, **8** and **9**.

A 5:1 variable plate impedance is possible, **Figure 7**, from just under 2 kΩ to as high as 10 kΩ. This provides a significant ability in gauging the proper termination load for the power amplifier. This is a simplified load pull arrangement. Notice there is a caveat. As the ZIN value rises towards 10 kΩ, so does the Qin. Hence, high unloaded Q components are a must as Qin of over 20 can compromise circuit efficiency if the unloaded Q is much less than 200. Note also the variation in the computed value of *C* tank, *Cp*. It tends to oscillate around 50 to 60 pF at a fixed frequency as the Qin variations force variations in the series loss added to the primary inductance, *L*1, see **(13)**. However, this is readily accommodated. Using a 180 pF capacitor in series with *L*2 resulted in an increase in output power of 3 dB.

Comparison to simulation

Using the spreadsheet calculation an array of series *C* elements is presented for a given value of measured link coupling parameters. The choice of a series tuned capacitor of 330 pF, see **Figure 10**, permits transferring a 50 Ω load to approximately 2 kΩ. Verification of this calculation is easy to accomplish in *LTspice* and the return loss, S11 and the transmission loss, S21 provide validation, **Figure 11**.

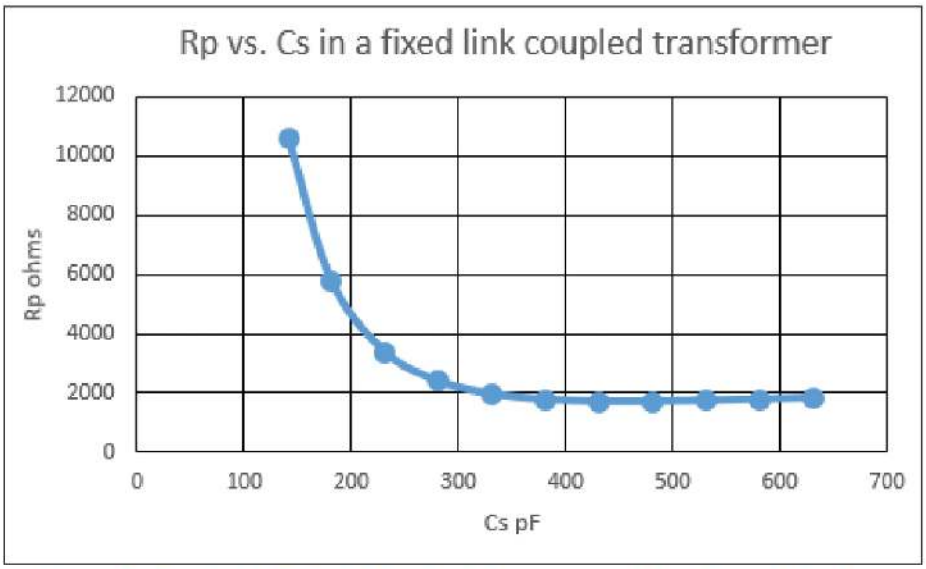

Figure 7 — Real part of ZIN, plate load resistance *vs.* secondary link coupled series capacitor *Cs*.

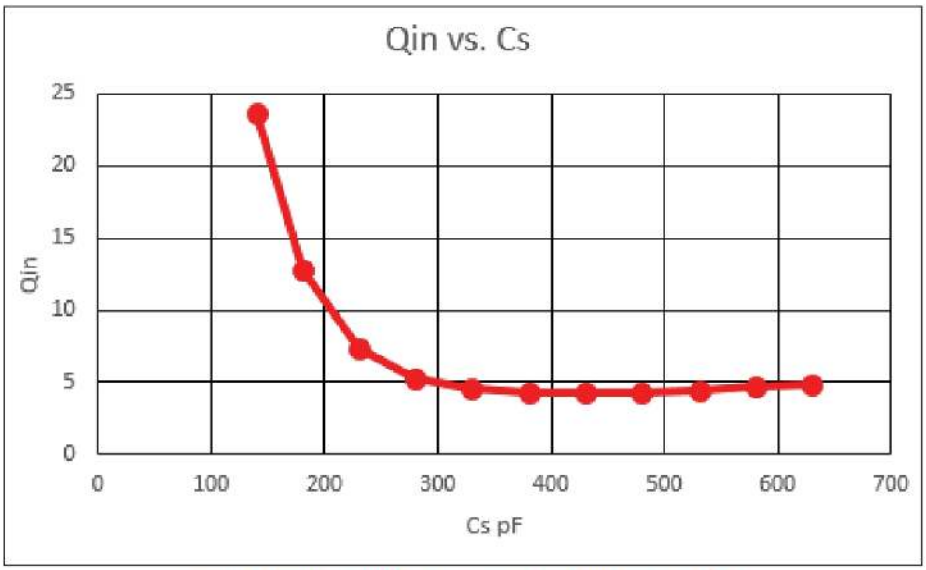

Figure 8 — Primary Qin *vs.* secondary link coupled *Cs*.

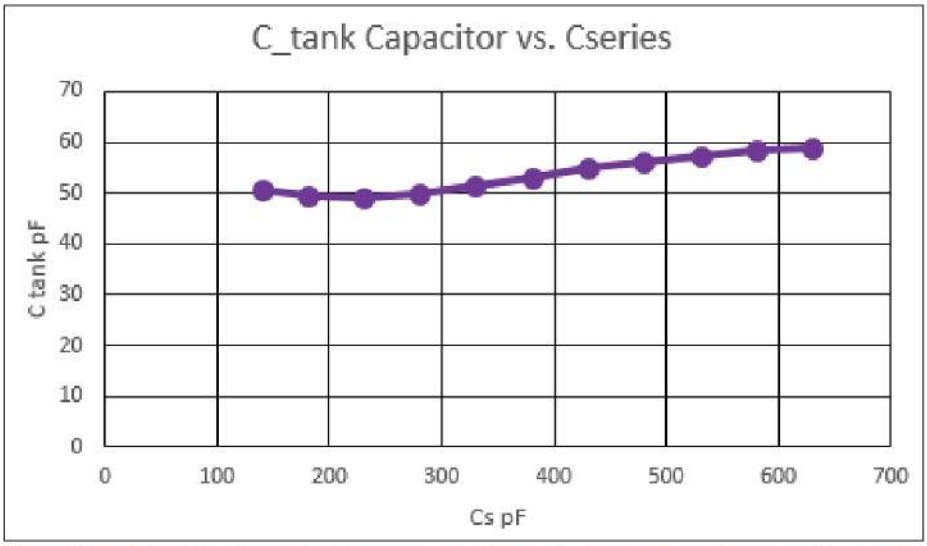

Figure 9 — Primary resonate tank capacitance, *Cp* *vs.* secondary coupling capacitance, *Cs*.

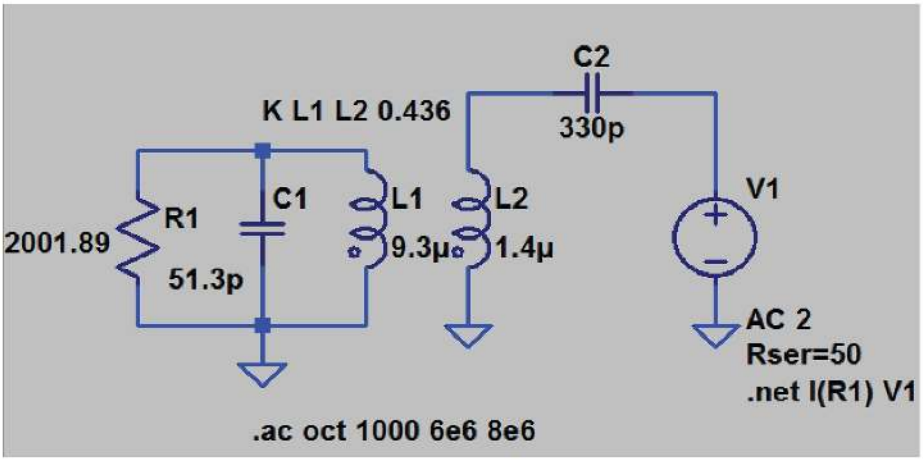

Figure 10 — From the spreadsheet sweep choose 330 pF for *Cs*. The remaining link coupled network parameters are as measured.

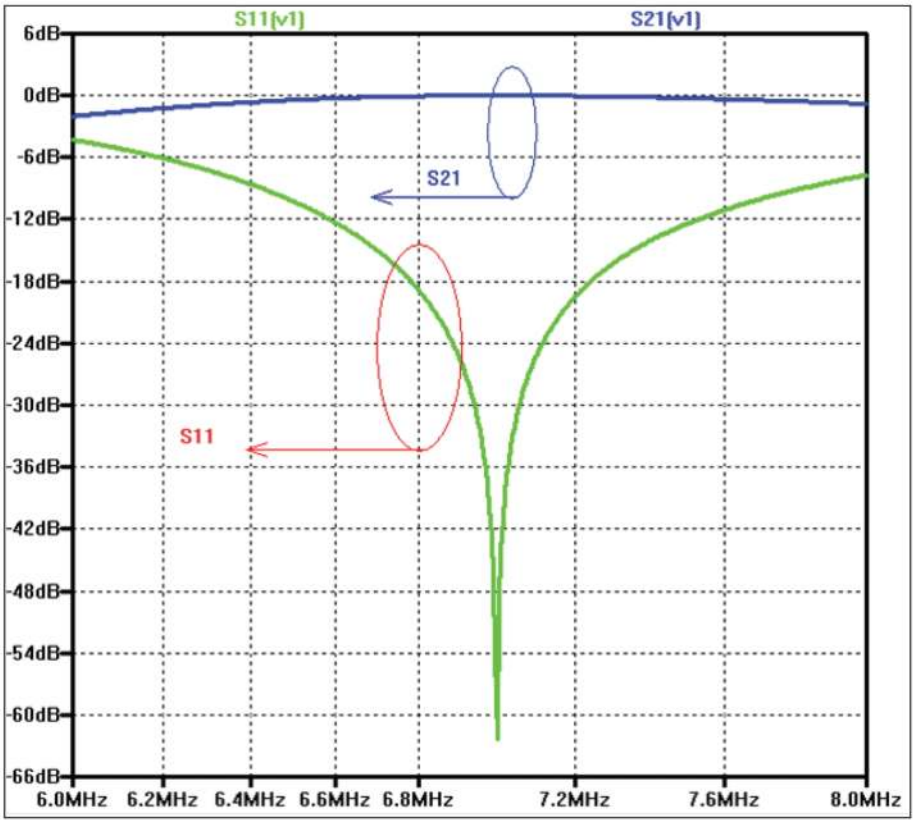

Figure 11 — The ZIN value is 2 kΩ and validation is clear as the return loss, S11, is greater than 60 dB. Qin is 4 and the bandwidth and insertion loss fall in line with the simulation for S21.

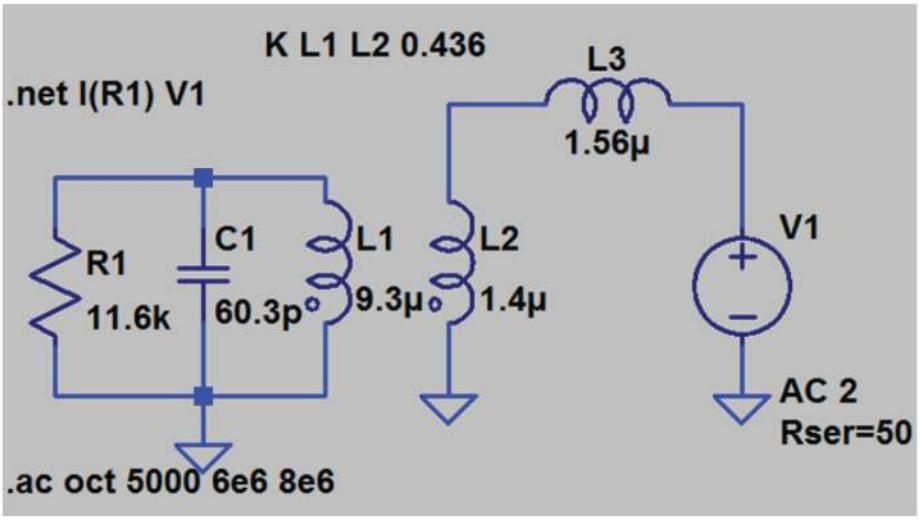

Figure 12 — Link coupled match obtained with a series coupling inductor.

Other possibilities

There is nothing restricting the application of a series inductive reactance with the load. This would be un-coupled from the primary. Since *Z* inversion takes place, the reflected *Z* is now series *XC* and *R*. This reflected series *XC* subtracts from the primary inductance reactance *XL*1 and again provides modification of ZIN with various values of series *Ls* with *L*2 on the secondary. As an example, a ZIN of nearly 12 kΩ is obtained if the coupling is a series *Ls* of 1.56 µH. The Qin is increased to 31 so the unloaded Q of the circuit elements must be maintained high to avoid significant insertion loss. See **Figure 12**, which implements this technique.

The ZIN value asymptotically approaches the *Cs* value where *Cs* is a dc block. That is to say, *Ls* approaches a short. The technique of adding series *Ls* on the secondary side is useful if the higher ZIN range is desired. However, the Qin needs to be in check to minimize network insertion loss. The frequency response transmission S21 is validated and the quality of match via the return loss or S11 is shown in **Figure 13**.

Figure 14 shows a homemade push-pull power amplifier using a link coupling with a variable output capacitor.

Conclusions

The transformer coupled tuned network is a versatile circuit topology. Its applications are diverse and some of the circuit subtle responses were discussed. The application as a simple load pull for push-pull circuits is discussed and this concept may be extended to solid state amplifiers as well as power oscillators and antenna tuners.

References

[1] W. B. Bruene, "How to Design R-F Coupling Circuits, Electronics," May 1952, pp. 134-139.

[2] A. Mazzanti, A. Bevilacqua, "Second-Order Equivalent Circuits for the Design of Doubly-Tuned Transformer Matching Networks," *IEEE Transactions on Circuits and Systems*, vol. 65, no. 12, pp. 4157-4168, Dec 2018.

[3] T.J. Maresca, W2VLA, "Simplified Design of Inductively-Coupled Circuits," *QST* Oct. 1959, pp. 29-31.

[4] An extensive discussion on the single tuned transformer is provided in Chapter 3, Section 3-5 of H. L. Krauss, C. W. Bostian, F. H. Raab, *Solid State Radio Engineering*, John Wiley and Sons, 1980.

[Photo by the author]

Alan Victor, W4AMV, was licensed in 1964. He operates mostly CW using an all homebrew station and enjoys design, construction and restoration of communication and test equipment. Alan worked in both the communication and semiconductor engineering fields. He received his PhD in electrical engineering from North Carolina State University and is currently involved with their mentorship program assisting new graduates in their engineering studies.

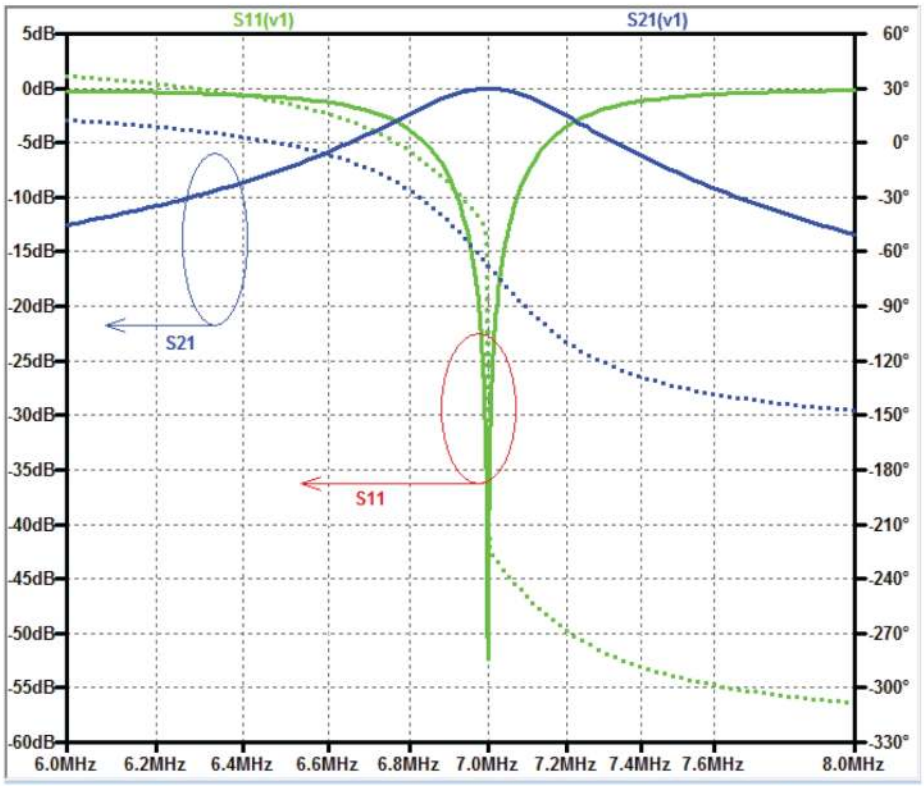

Figure 13 — The frequency response, transmission S21 and the return loss S11 for the link coupled circuit of Figure 12. The series element to the coupling link is an inductor. The S21 and S11 response are excellent and in agreement with calculation.

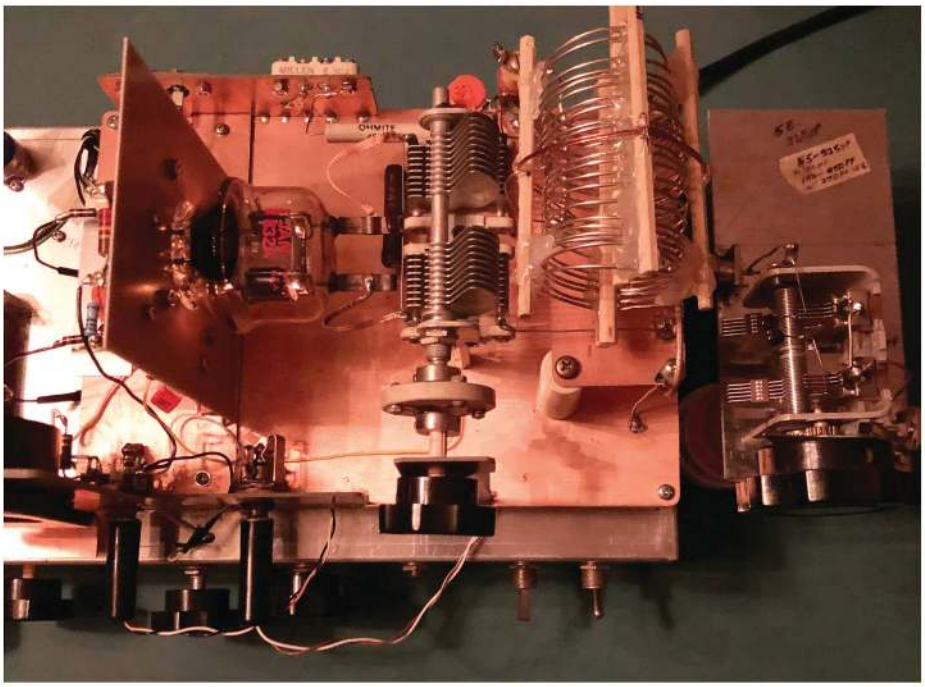

Figure 14 — Homemade push-pull power amplifier using a link coupling with a variable output capacitor.

Eric P. Nichols, KL7AJ

AlasKit Educational and Scientific Resources, 3763 Lyle Ave., North Pole, AK 99705; **kl7aj72@gmail.com**

Self-Paced Essays — #9 Angular Frequency

Essay 9: Expanding mathematical concepts into ac circuits.

In the preceding eight essays we laid out a fairly complete foundation for dc electronics. This is not to imply that we won't be returning to dc circuits many times throughout this series, because we will. But with a solid understanding of Ohm's Law and Kirchhoff's Laws, we can now expand these concepts to alternating current (ac) circuits at all frequencies.

We warned you earlier that all those mathematics concepts that you may have skimmed over in your earlier education — we believe *most* of our readers are mid-career or later — will come back to haunt you in this series. One of those elusive math concepts is the *radian.*

Allow me to speak first to the "well-seasoned" radio practitioners in our midst, and then return promptly to those for whom this is entirely new. We do want to be sure everyone is on the same level playing field, before we move on too far.

If you've been a radio amateur or electronics technician for any length of time, you are well familiar with the concept of *frequency,* usually measured in cycles per second, or *hertz.* Most of us in Western society naturally think of directional or rotational measurements in terms of *degrees* and subdivisions of degrees. Here are interesting passages on the degree from *Wikipedia*:

The original motivation for choosing the degree as a unit of rotations and angles is unknown. One theory states that it is related to the fact that 360 is approximately the number of days in a year. Ancient astronomers noticed that the sun, which follows through the ecliptic path over the course of the year, seems to advance in its path by approximately one degree each day. Some ancient calendars, such as the Persian calendar and the Babylonian calendar, used 360 days for a year. The use of a calendar with 360 days may be related to the use of sexagesimal numbers.

Another theory is that the Babylonians subdivided the circle using the angle of an equilateral triangle as the basic unit, and further subdivided the latter into 60 parts following their sexagesimal numeric system The earliest trigonometry, used by the Babylonian astronomers and their Greek successors, was based on chords of a circle. A chord of length equal to the radius made a natural base quantity. One sixtieth of this, using their standard sexagesimal divisions, was a degree.

Aristarchus of Samos and Hipparchus seem to have been among the first Greek scientists to exploit Babylonian astronomical knowledge and techniques systematically. Timocharis, Aristarchus, Aristillus, Archimedes, and Hipparchus were the first Greeks known to divide the circle in 360 degrees of 60 arc minutes. Eratosthenes used a simpler sexagesimal system dividing a circle into 60 parts.

The division of the circle into 360 parts also occurred in ancient India, as evidenced in the Rigveda:

Twelve spokes, one wheel, navels three.
Who can comprehend this?
On it are placed together
three hundred and sixty like pegs.
They shake not in the least.
—Dirghatamas, Rigveda 1.164.48.

The problem is that the degree is, surprisingly, not an SI standard unit. It is an accepted unit by SI, but not an actual standard. Please re-read the Essay 3 sidebar, "Raising a Standard or Two." On the other hand, the radian is indeed an SI unit. For most of this series we will use the radian-derived angular frequency, not to be annoying, but because it greatly condenses and simplifies a lot of ac analysis, especially when we eventually move into Fourier Analysis.

Now, back to our newcomers, as promised. Since this essay series is primarily geared as an on-ramp to genuine electrical engineering, we might as well get in the habit of using real engineering standards right out of the chute. Although "normal" frequency is intuitive to most electronics technicians, angular frequency will become quite natural with practice, and will actually give you some additional insights and perhaps an "aha moment" or two.

What It Is

With the assumption that a complete circle is 360°, we might define a radian as 57.2958°. But there are two levels of error in this "definition." First of all, 57.2958° is truncated, there are a whole lot of decimal places after this. Secondly, the degree itself is not even a standard, as explained above. So, just like using calculations that require π, or some such identity, we should use concrete identities when working with angular measurements. By angular here, we don't necessarily mean physical angles, but they can also be electrical phase angles. In most of our discussions, that is the kind of angle with which we'll be dealing.

So, where does this 57.2958 come from, anyway? It's common practice to round this figure up to 57.3, while most scientific calculators will give you 57.29577951 as the final answer. Well, if we divide a circle by π, we find that we have $2\pi \times 57.3°$

in said circle. At first, this may seem immensely inconvenient. However, as we will learn before too long, by dividing up a circle into discrete "chunks" of π we can have extremely accurate and, more importantly, *useful* fractions of a circle, without the inherent error of referring to degrees. In working with ac, we find that several fundamental identities fit perfectly into $\pi/2$ radians, which is a perfect right angle, or 90°. Remember, degrees are not fundamental units, but radians are.

Incidentally, this might be a good time to set up your scientific calculator to display answers in radians, as those will be our default units for most of our future discussions. This might also be a good time to figure out exactly what order of operations your calculator performs. This is *not* absolutely consistent between different manufacturers of calculators. Many of my students learned this the hard way, in the midst of either a commercial or amateur radio exam. Don't let this happen to you! Work out a few test problems requiring multiple operations so you *know* precisely how your calculator behaves.

Now, if we were to define a cycle as one complete repetition of a repetitive waveform — commonly a sine wave — we will have precisely 2π radians per lap around the circle. We can define the frequency of a repetitive waveform in terms of cycles, or laps in a fixed unit of time, commonly a second. If we establish one cycle as 2π radians and our frequency as one second, we can come up with a very useful entity known as the unit angular frequency ω always expressed in radians: $\omega=2\pi f$.

Dimensionless

In mathematics and most sciences, we have certain identities that are exact ratios of two different entities. Take for instance, the ratio of the circumference of a circle to its diameter. This ratio is equal to π. We can assign units to both the circumference and the diameter, preferably the same units. Assigning a unit to a measurement implies a certain dimension. If the diameter is one foot, the circumference is 3.14159… feet. These are both measurements of length.

We know that *Diameter/Circumference* = π, regardless of the units of the two original lengths, again, assuming they are the same units. However, we can cancel out the actual units in our circle, and come out with just π, which is a dimensionless unit. By doing away with the dimensional units, by simple cancellation, we can simplify a lot of formulas and equations.

In like manner angular frequency π can often be treated as a dimensionless unit, simplifying the normal equations for reactance, impedance, and resonant frequency.

Chunks

One of the conveniences of using radian-based measurements becomes readily apparent when working with phase angles, which we will explore before long. As it turns out, many physical phenomena involve quadrature or orthogonal quantities, that is, quantities that are exactly 90° apart in either time or space. $\pi/2$ radians is exactly 90°; which is exactly the phase shift incurred by either a capacitor or an inductor. Another common phase angle is $\pi/4$, or 45°.

These common "chunks" of phase angles: 45°, 90°, 135°, 180°, 225°, 270°, 315°, and 360° are most conveniently expressed in radial fashion: $\pi/4$, $\pi/2$, $3\pi/4$, π, $5\pi/4$, $3\pi/2$, $7\pi/4$, and 2π. Again, these are very precise fundamental definitions, unlike our highly-derived degrees. So it's best to begin thinking in radian terms from the very beginning of our journey into ac electronics.

Dimensional Analysis

In cases where we do need to work with actual units, it's important that we perform mathematical operations on dimensionally equivalent units. In other words, we must compare apples to apples and oranges to oranges. There's an entire branch of math known as dimensional analysis, which explores the "common dimensionality" or lack thereof of many advanced and complex physical phenomena. In many cases, two measurements are obviously dimensionally equivalent, but in many cases, it's not so obvious.

As an obvious demonstration, an inch and a foot are dimensionally equivalent, while a foot and a year are not dimensionally equivalent.

In ac electronics, we will be working with values such as capacitance (measured in farad), or inductance, (measured in henry). However, we will also be working with capacitive and inductive reactances, respectively, which are measured in ohms. Capacitance is not dimensionally equivalent to capacitive reactance, but capacitive reactance is dimensionally equivalent to resistance. A fairly reliable hint that measurements are dimensionally equivalent is that they have the same units.

If you get in the habit of always writing the units down next to any calculation, you will avoid dimensional mismatching, which is a very common error of both beginning engineering students and some of us old timers at times. I know it can seem tedious in the midst of a long, multistep calculation, but trust me, it will save you a lot of trouble later on!

Upcoming Conferences

8th Annual TECHCON — 2022

February 25 – 26, 2022

Winter Haven, Florida

http://arrlwcf.org/wcf-special-events/wcftechconference/

The 8th Annual TECHCON, the ARRL West Central Florida Section Technical Conference, will be held February 25 – 26, 2022, at the Polk County EOC, 1890 Jim Keene Blvd., Winter Haven, FL. See website for details.

SCALE 19x

March 3 – 6, 2022

Pasadena, California

www.socallinuxexpo.org/scale/19x

SCALE 19x, the 19th annual Southern California Linux Expo, will take place March 3 – 6, 2022, at the Pasadena Convention Center. SCALE is the largest community-run open-source and free software conference in North America. It is held annually in the greater Los Angeles area. See website for details.

Technical Note

Mesh Analysis Homework Solution for Essay 6

In Essay 6 (*QEX* May/June 2021) we presented a homework problem. I was extremely gratified with the response. We received a lot of really good emails, and I have tried to answer them individually. The emails contained comments like, "I learned this stuff 50 years ago and forgot it all; thanks for the reminder!"

In light of this, I thought it would be most informative to dissect the gold star solution provided by Mike Newland, N4JRG, see **Figure 1**. His solution isn't necessarily the simplest or the only way, but I'd consider it the "safest" in that, to the best of my knowledge, it will always work. It also gives us a nice introduction to classical *mesh analysis*.

Mike uses *conventional current flow* to solve this, where current flows from the positive source to the negative source. Electrical engineers tend to favor conventional current flow, while technicians generally use the *electron* flow, which goes in the opposite direction. Either convention is just fine as long as you're absolutely consistent.

Mike notes that mesh analysis is his "go to" method of solving these problems, and I agree. We've had readers also suggest creating Norton and Thévenin equivalent circuits, another powerful tool we will cover later in this series. There is always more than one way to solve any electrical problem, and all of them can be very good!

Recall from Essay 7, where we suggested that, when solving complex circuits, it's a good idea to build a table showing every component in a circuit along with a list of everything we know about each component. This is especially useful when working with mesh problems. This practice will sometimes give you more information than you need to know, but it's better to have more than you need than less than you need. We don't need to go into the tedium of creating the table here, which we will leave for an exercise. For all practical purposes, Mike has done this task for us.

First, he sets up two *mesh* equations, each of which satisfies Kirchhoff's Voltage Law (KVL). A *mesh* is simply two interconnected loops, or more concisely, loops that share a common component.

Mesh 1: $-12 + 100i_1 + 100(i_1 + i_2) = 0$

Mesh 2: $-12 + 100i_2 + 100(i_1 + i_2) = 0$.

Collecting the terms and rearranging to get rid of the zeroes gives us,

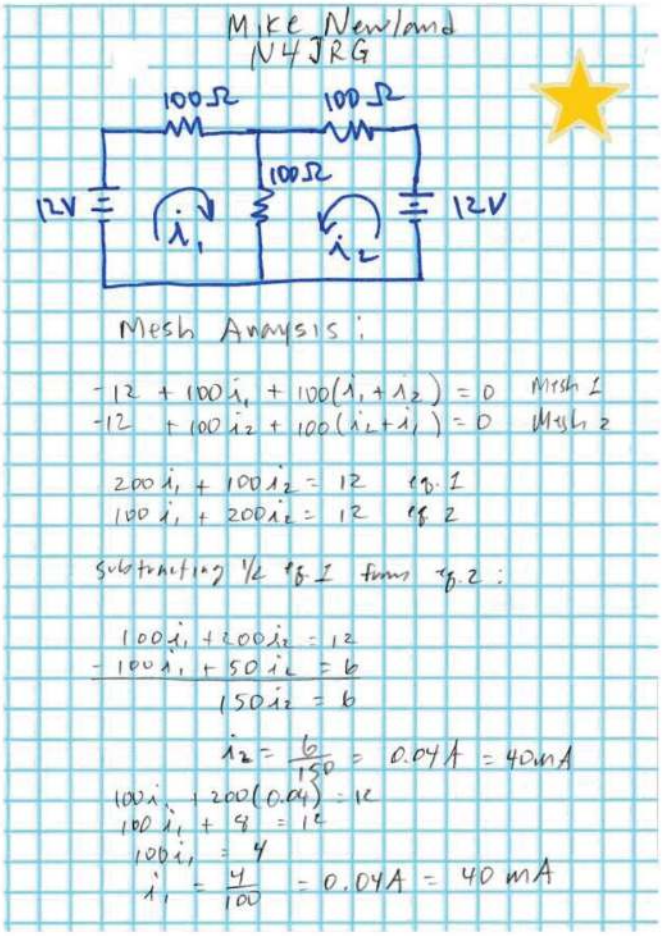

Figure 1 — Homework solution by Mike Newland, N4JRG.

Eqn(1): $200i_1 + 100i_2 = 12$

Eqn(2): $100i_1 + 200i_2 = 12$.

Now we have to solve two simultaneous equations, something from our high school years we all forgot how to do. We said before that everything you ever learned in high school math would come back to haunt you; here it is!

Mike divides Eqn(1) by two and subtracts it from the Eqn(2),

$100i_1 + 200i_2 = 12$

$-(100i_1 + 50i_2 = 6)$

which yields $150i_2 = 6$. Solving for i_2, we get 6/150 or 0.04 A.

We know i_1 must equal to i_2 and, by Kirchhoff's Current Law (KCL), we know that the current through the center resistor connected to ground must be $i_1 + i_2$ or 0.08 A. Thus the voltage across the center resistor is 0.08 × 100 = 8 V, the final answer. Mike gets a gold star for NOT assuming that i_2 and i_1 are the same, and carrying out the second substitution in our simultaneous equation, a step beyond the call of duty.

Several of you asked about my simple "cheat." Yes it is legal, and here it is. If you connect a wire between the two equal "+" sources (node 1 and node 2), this places the two top resistors in parallel (as well as doing the same for voltage sources), converting this to a very simple voltage divider problem. This is fine as long as the two connected nodes are at the same potential; the added wire has no effect on the circuit operation. This is true for any circuit, no matter how complex. This is the principle of "virtual shorts," which becomes very useful in many active circuits containing op-amps and the like.

I'm a big fan of the Socratic method of teaching; allowing my students to teach each other, rather than me merely pontificating from the front of the class. Thanks, Mike! — *Best regards, Eric P. Nichols, KL7AJ,* **kl7aj72@gmail.com**.

Send your short *QEX* Technical Note to the Editor, via e-mail to qex@arrl.org. We reserve the right to edit your letter for clarity, and to fit in the available page space. "*QEX* Technical Note" may also appear in other ARRL media. The publishers of *QEX* assume no responsibilities for statements made by correspondents.

2021 *QEX* Index

Great New Gear for the New Year at DX Engineering!

YAESU

Yaesu FTM-6000R 50W 144/430MHz Dual Band FM Mobile Transceiver

This feature-rich and easy-to-operate rig delivers 50 watts of transmit performance, 3 watts of crisp and clear audio specifically tuned for radio communication, detachable monochrome display front panel that you can mount for maximum convenience, three user-intuitive operating modes, and the ability to activate favorite assigned functions with a single touch. Enjoy hands-free wireless operation with the optional Yaesu BU-4 Bluetooth® adapter plug-in module and SSM-BT10 Bluetooth headset.
Enter "FTM-6000R" at DXEngineering.com.

RADIOANALOG

innovations that excite radio enthusiasts

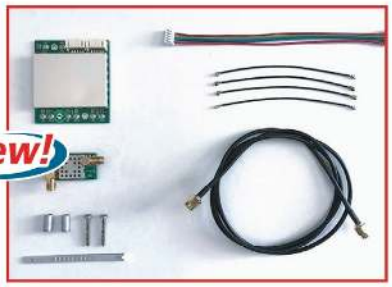

Panadapter IF Interface Module for Icom IC-9700 Transceiver

On the heels of Radio Analog's PTRX-7300-V2 panadapter module for the IC-7300 comes its new model that lets you view the IC-9700's panadapter in an easier-to-see, larger-screen format when combined with your external SDR receiver. Designed for exceptional performance and hassle-free installation in minutes (with no modification needed at the rig's rear panel, no compromise in the radio's performance, and no soldering or special skills required), the PTRX-9700 can be installed using only a screwdriver and provided special tool.
Enter "PTRX-9700" at DXEngineering.com.

NanoVNA-F V2 Vector Network Analyzer

Used for recording a variety of RF measurements from 50 kHz to 3 GHz (S parameters, VSWR, Smith chart, phase, group delay, and more), this handy and versatile device features a 4.3" IPS LCD display, 5000mAh large-capacity lithium battery, RG405 phase-stable cable, SMA port, standard USB port for easy charging, simple firmware upgrades, and frequency accuracy of <0.5ppm. It comes housed in a sturdy aluminum alloy case to ensure precise measurements by shielding electromagnetic interference.
Enter "NanoVNA" at DXEngineering.com.

YAESU

Yaesu FT5DR 2m/70cm C4FM/FM Digital Handheld Transceiver

Kick off 2022 by adding this powerful new rig to your collection. Lightweight, compact and rugged, the FT5DR provides reliable 5 watts of RF power output, wide-range RX coverage, loud and clear analog FM and digital C4FM voice quality, two independent receivers that support true dual-band operation, high-resolution display, real-time monitoring with the Band Scope function, shock-resistant construction with an upgraded IPX7 waterproof rating, and loads more.
Enter "FT5DR" at DXEngineering.com.

COMPAC tenna

CompacCounterpoise NMO Mount Base Station Ground Plane

This kit turns your COMPACtenna antennas into sturdy and stealthy base stations. Add the provided radials to optimize signals and SWR for UHF/VHF operation, with a maximum power rating of 250 watts (up to 225 MHz) and 100 watts on higher frequencies. The kit comes with 3" diameter mounting plate with mast bracket, clamps, four 18" radials, and stainless steel hardware. It works with many monoband or multiband NMO-mount antennas, including COMPACtenna's 2M-440, 2M-220-440, SCAN-III, and the new LMR-I Land Mobile Radio Antenna designed for government and commercial applications.
Enter "CompacCounterpoise" at DXEngineering.com.

kelemen Antennas

DX Engineering is excited to be the exclusive North American retailer of high-performance, finely constructed Kelemen wire antennas from WiMo. Choose from more than 50 models of high-efficiency, wide-bandwidth monoband or multiband dipoles and omni-directional antennas in a range of supported bands, lengths, and power ratings (200W to 2,000W). Antennas come assembled with balun.
Enter "Kelemen" at DXEngineering.com.

ON ALL BANDS

DX Engineering's Amateur Radio Blog for New and Experienced Hams.

Need a Custom Cable? Custom Cables Ship in One Business Day!

DX® ENGINEERING

Ordering (via phone) Country Code: +1
9 am to midnight ET, Monday-Friday
9 am to 5 pm ET, Weekends

Phone or e-mail Tech Support: 330-572-3200
9 am to 7 pm ET, Monday-Friday
9 am to 5 pm ET, Saturday

Ohio Curbside Pickup:
9 am to 8 pm ET, Monday-Saturday
9 am to 7 pm ET, Sunday

Nevada Curbside Pickup:
9 am to 7 pm PT, Monday-Sunday

800-777-0703 | DXEngineering.com

ON ALL BANDS YouTube

We're All Elmers Here! Ask us at: Elmer@DXEngineering.com
Email Support 24/7/365 at DXEngineering@DXEngineering.com

SOLAR CYCLE 25

IS HERE... AND WE HAVE THE GOODS TO ENJOY IT!

Sunspot Cycle 25 could have a magnitude that rivals the top few since records began. There is a 95% chance that Cycle 25 amplitude will fall between 153 and 305 spots, and with 68% confidence that the amplitude will be 233 spots. More sunspots during a cycle's solar maximum means better skip propagation, improved DXing, more log books filled with never-thought-possible QSOs, and happier Hams.

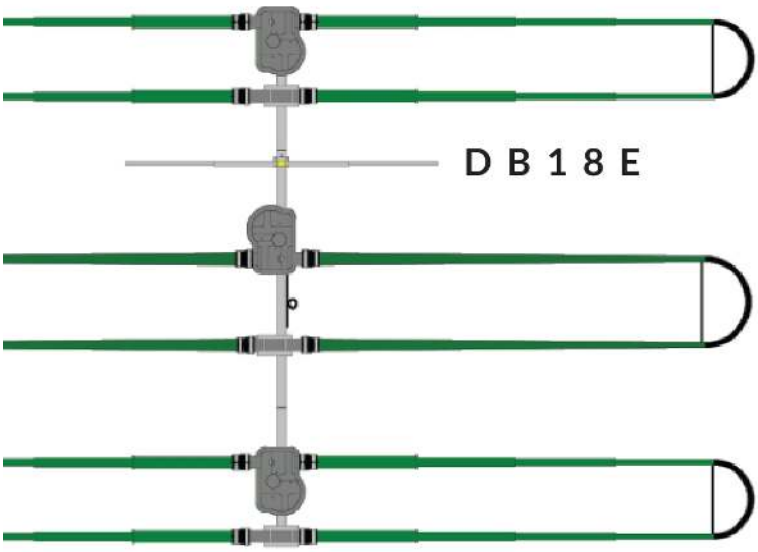

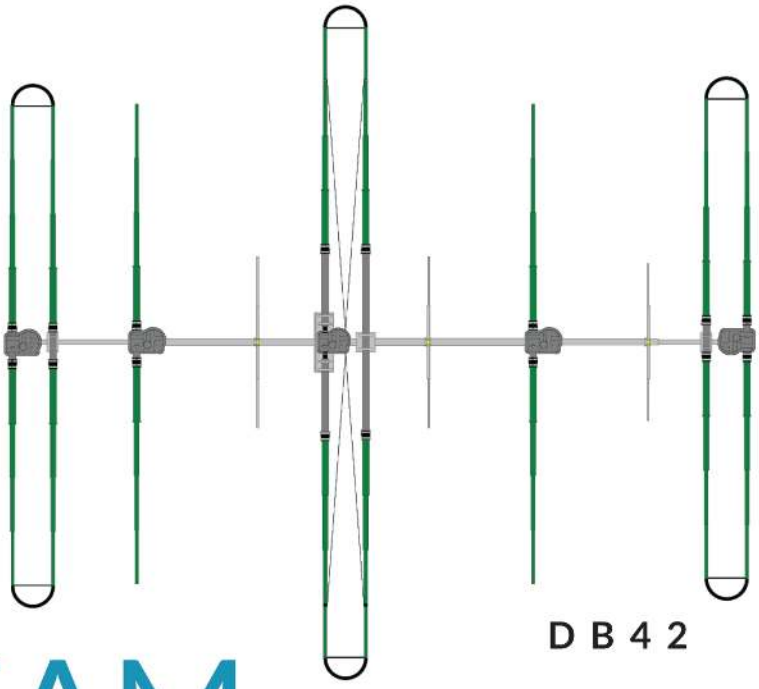

DREAM BEAM

The DB Series (DreamBeam) Yagi antennas are ideal for those looking for broadband, high-performance gain and exceptional front-to-rear. Each DreamBeam, with the exception of the ultra-stealth DB-11 (13.8-54 MHz), is an optimized Yagi antenna 6.8-54 MHz. The DB36 and DB42 Yagis have 3.5 -6.8 MHz dipole options available, which utilize the end elements as top-hats for excellent band coverage. All of the DB Series antennas employ our patented loop technology, resulting in a physical footprint that is 40% shorter than a full-size Yagi – with only 0.3 dB reduction in performance gain!

ANTENNA SYSTEMS

steppIR COMMUNICATION SYSTEMS

FOR PRODUCT DETAILS AND ORDERING:

www.steppir.com

425-453-1910

20TH ANNIVERSARY steppIR